



Research paper

Design and characterization of cereblon-mediated androgen receptor proteolysis-targeting chimeras



Akshay D. Takwale ^{a, b, 1}, Seung-Hyun Jo ^{e, f, 1}, Yeong Uk Jeon ^a, Hyung Soo Kim ^c, Choong Hoon Shin ^d, Heung Kyoung Lee ^a, Sunjoo Ahn ^a, Chong Ock Lee ^a, Jae Du Ha ^{a, **}, Jeong-Hoon Kim ^{e, f, ***}, Jong Yeon Hwang ^{a, b, *}

^a Therapeutics and Biotechnology Division, Korea Research Institute of Chemical Technology, Daejeon, 305-606, Republic of Korea

^b Department of Medicinal Chemistry and Pharmacology, Korea University of Science and Technology, Daejeon, 34113, Republic of Korea

^c Department of Chemistry, Korea University, Seoul, 02841, Republic of Korea

^d Department of Chemistry, Sogang University, Seoul, 04107, Republic of Korea

^e Disease Target Structure Research Center, Korea Research Institute of Bioscience and Biotechnology, Daejeon, 34141, Republic of Korea

^f Department of Functional Genomics, Korea University of Science and Technology, Daejeon, 34113, Republic of Korea

ARTICLE INFO

Article history:

Received 14 May 2020

Received in revised form

13 August 2020

Accepted 14 August 2020

Available online 26 August 2020

Keywords:

Androgen receptor

Proteolysis targeting chimera

Prostate cancer

Cereblon

TD-106

ABSTRACT

Proteolysis-targeting chimera (PROTAC)-mediated protein degradation is a rapidly emerging therapeutic intervention that induces the degradation of targeted proteins. Herein, we report the design and biological evaluation of a series of androgen receptor (AR) PROTAC degraders for the treatment of metastatic castration-resistant prostate cancer. Predominantly, instead of thalidomide, we utilized the TD-106 scaffold, a novel cereblon (CRBN) binder that was identified in our previous study. Our results suggest that the linker position in the TD-106 CRBN binder is critical for the efficiency of AR degradation. The compounds attached to the 6-position of TD-106 promoted better degradation of AR than those at the 5- and 7-positions. Among the synthesized AR PROTACs, the representative degrader **33c** (TD-802) effectively induced AR protein degradation, with a degradation concentration 50% of 12.5 nM and a maximum degradation of 93% in LNCaP prostate cancer cells. Additionally, most AR PROTAC degraders, including TD-802, displayed good liver microsomal stability and *in vivo* pharmacokinetic properties. Finally, we showed that TD-802 effectively inhibited tumor growth in an *in vivo* xenograft study.

© 2020 Elsevier Ltd. All rights reserved.

1. Introduction

The androgen receptor (AR), a member of the nuclear hormone receptor superfamily, plays a vital role in the maintenance of male secondary sexual characteristics and development of the prostate gland. Upon binding to its natural ligand, dihydrotestosterone, AR regulates target gene transcription [1–4]. Besides its role in downstream signaling, AR is required for prostate cancer growth;

therefore, AR is a major target for prostate cancer therapies. Several techniques, such as androgen deprivation therapy by castration and radiotherapy, are used as a standard of treatment [5,6]. Anti-androgen small molecules (Fig. 1), including enzalutamide (**1**) and apalutamide, which inhibit ligand binding to AR, are currently used to treat AR-dependent prostate cancer [7–9]. Although anti-androgen drugs are available, side effects as well as resistance progressing to metastatic castration-resistant prostate cancer (mCRPC) have been observed with these treatments, necessitating novel anti-androgen modalities [10]. Targeted protein degradation is a rapidly emerging therapeutic intervention that induces protein degradation. Proteolysis-targeting chimera (PROTAC) is a hetero-bifunctional molecule composed of a binder for target protein binding, a binder for E3 ubiquitin ligase binding, and a linker for connecting two binders [11]. PROTAC promotes the formation of a ternary complex with the targeted protein and E3 ligase, leading to ubiquitination of the targeted protein and subsequent proteasomal

* Corresponding author. Therapeutics and Biotechnology Division, Korea Research Institute of Chemical Technology, Daejeon, 305-606, Republic of Korea.

** Corresponding author.

*** Corresponding author. Disease Target Structure Research Center, Korea Research Institute of Bioscience and Biotechnology, Daejeon, 4141, Republic of Korea.

E-mail addresses: jdha@kriict.re.kr (J. Du Ha), jhoonkim@kribb.re.kr (J.-H. Kim), jyhwang@kriict.re.kr (J.Y. Hwang).

¹ These authors contributed equally to this study.

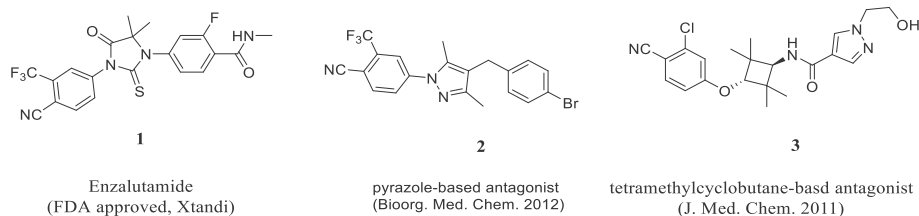


Fig. 1. Chemical structure of the reported androgen receptor (AR) antagonists.

degradation process. Currently, several E3 ubiquitin ligases, including b-TRCP, MDM2, cIAP, VHL, and cereblon (CRBN), have been used in PROTAC [12,13]. Among these, cIAP, VHL, and CRBN have been successfully applied in the degradation of various targets such as FKBP12, ER α , AR, BET, BCR-ABL, and RIPK2 [14–20].

Several groups have reported AR PROTAC degraders (Fig. 2). ARV-110, developed by Arvinas, is the first clinical trial of a PROTAC degrader for the treatment of patients with mCRPC [21]; however, its structure remains unknown. Naito et al. have reported AR degrader **4** by applying their targeted protein degradation platform, named specific and nongenetic inhibitor of apoptosis protein (IAP)-dependent protein erasers, for E3 ligase and pyrazole-based AR antagonist **2** [22]. Furthermore, Crews et al. have reported AR degrader **5** (ARCC-4), which utilizes a VHL ligand for the E3 ligase and enzalutamide as the AR antagonist [23]. Recently, Wang et al. have reported two degraders, **6** (ARD-69) and **7** (ARD-266), using VHL ligands and tetramethylcyclobutane-based AR antagonist **3**. They systematically explored the effect of linkers and inhibitors, and E3 ligases, achieving highly potent AR degraders with degradation concentration 50% (DC₅₀) values in the low nanomolar ranges. Additionally, a single dose of ARD-69 effectively decreases the number of AR in tumor tissues of xenograft mice [24].

Previously, we reported the novel CRBN binder **8** (TD-106) that binds to CRBN and induces efficient degradation of well-known neosubstrates, IKZF1/3. Moreover, we successfully validated its applicability for PROTAC degraders, inducing BET protein degradation [25]. As part of our efforts to develop targeted protein degradation programs, we were interested in generating an effective AR PROTAC degrader mediated by TD-106 CRBN binder. Although highly potent AR PROTAC degraders have been reported, as mentioned above, no potent AR PROTAC degrader utilizing thalidomide analogs to recruit CRBN E3 ligase has been reported. Wang et al. reported only two compounds with very weak or no degradation in LNCaP cells [24]. Moreover, *in vivo* antitumor

efficacy data of AR PROTAC have not been reported. The potency of PROTAC is generally influenced by the use of the E3 ligase, linker, and warhead independently. Therefore, we hypothesized that AR PROTACs utilizing TD-106 as a CRBN binder can provide effective AR degradation. Herein, we report the synthesis of AR degraders with TD-106 and results from biological evaluations performed *in vitro* and *in vivo*.

2. Results and discussion

2.1. Design and synthesis of AR-PROTAC

To generate a successful PROTAC degrader, the attachment of the linker to the warhead, as well as the type of linker, is critical. Although the X-ray co-crystal structure of the AR ligand-binding domain with antagonist **3** has not been reported, we utilized the molecular docking model of antagonist **3** published by Guo et al. [26] as well as the AR co-crystal structure with agonists [27]. We replaced the pyrazole-hydroxyethyl moiety of **3** with phenyl-piperazine as an exit vector, as reported previously, as it was exposed to solvent and was well-tolerated for structural modifications, making it suitable for conjugation to a CRBN ligand via linkers (Fig. 3) [26]. For CRBN binding, we also explored the position of the linkage at TD-106, particularly at the 5-, 6-, and 7-positions.

Tetramethylcyclobutane-based AR antagonist **15** was prepared from ethyl 4-fluorobenzoate **10** using a modified method, as shown in Scheme 1. Briefly, acid **12** was prepared from starting material **10** by a substitution reaction with *tert*-butyl piperazine-1-carboxylate, followed by hydrolysis. Amide coupling with intermediate **13**, prepared as previously described [26], provided **14**, which was transformed to the desired AR binder **15** by treatment with hydrogen chloride.

CRBN binders **18**, **20**, and **26** were synthesized as shown in

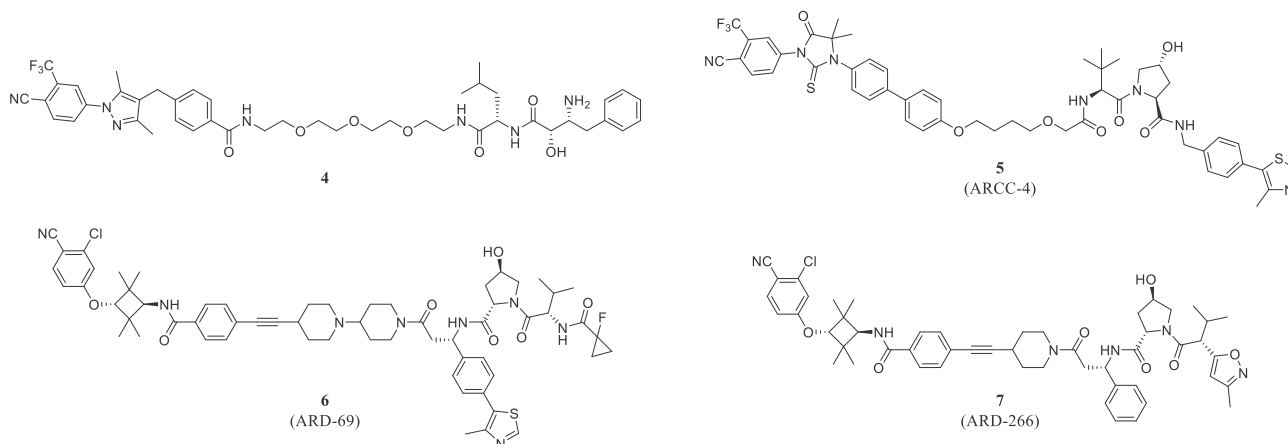


Fig. 2. Chemical structure of the reported androgen receptor (AR) degraders.

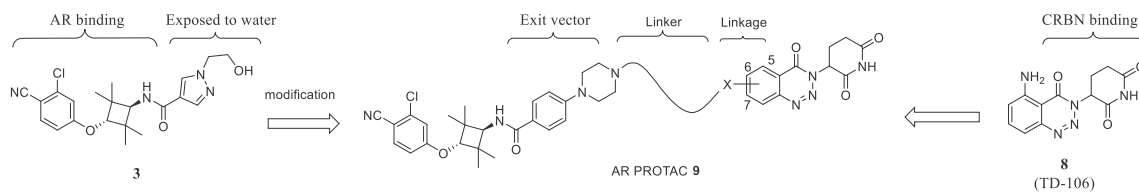
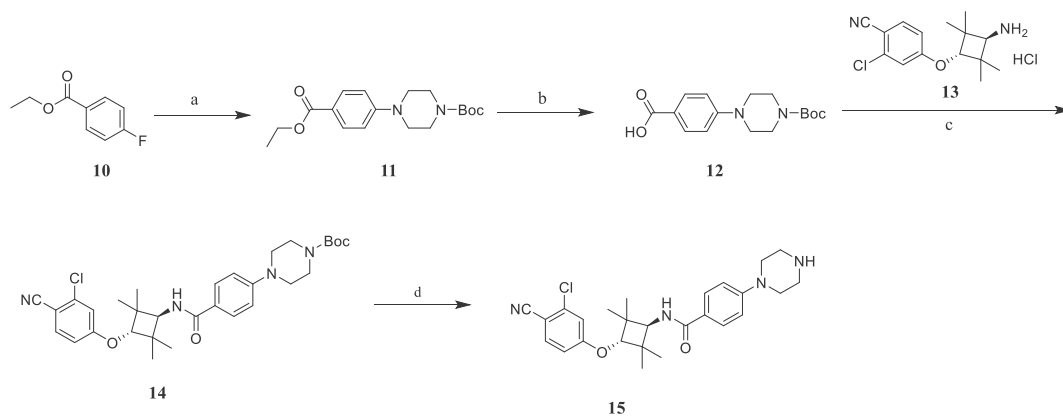
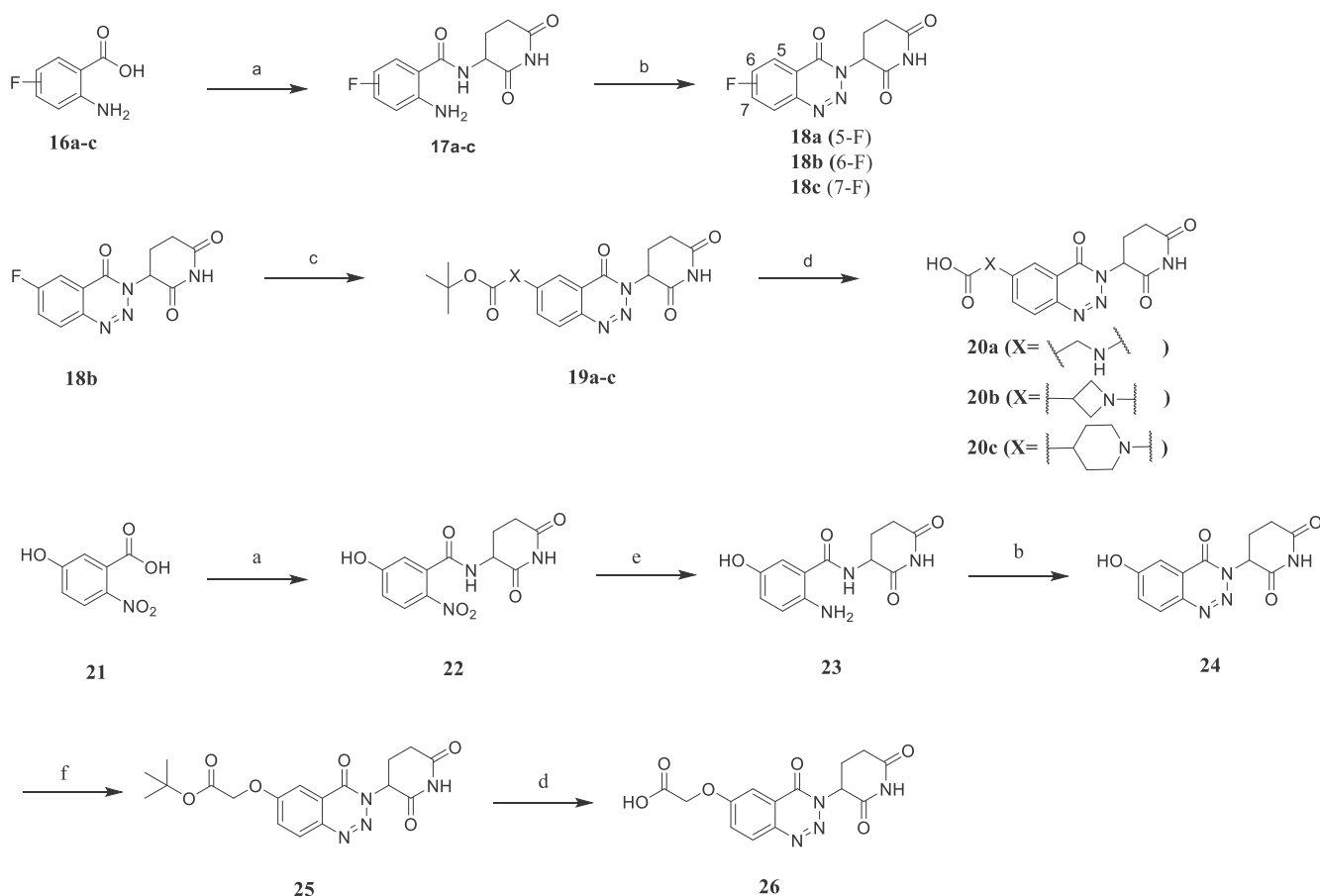


Fig. 3. Strategy for the tethering androgen receptor (AR) antagonist (**3**) and cereblon (CRBN) binder (**8**) in this study.



Scheme 1. Reagents and conditions; (a) DIPEA, DMSO, *tert*-butyl piperazine-1-carboxylate, 130 °C; (b) LiOH·H₂O, THF, H₂O, MeOH, 40 °C; (c) EDCI, HOBT, DIPEA, **13**, DMF, room temperature (rt); (d) 4.0 M HCl in dioxane, DCM, rt.



Scheme 2. Reagents and conditions: (a) EDCI, HOBT, DIPEA, 3-aminopiperidine-2,6-dione hydrochloride, DMF, room temperature (rt); (b) NaNO₂, AcOH, rt; (c) DIPEA, DMF, 17, 90 °C; (d) TFA:DCM (1:1), rt. (e) Pd/C, H₂, MeOH; (f) K₂CO₃, *tert*-butyl-2-bromoacetate, DMF, rt.

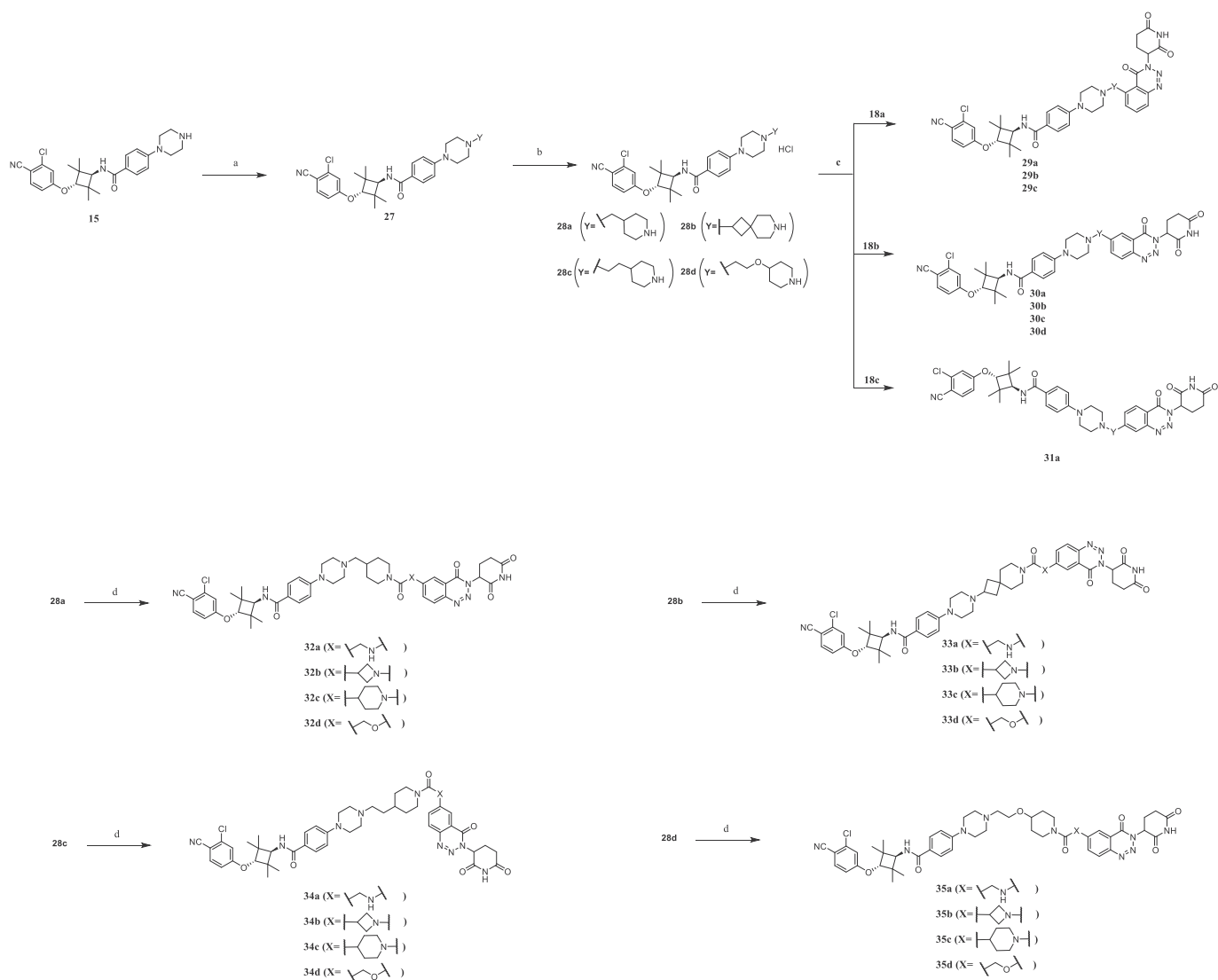
Scheme 2. Fluoro-substituted 2-aminobenzoic acid **16** was treated with 3-aminopiperidine-2,6-dione hydrochloride in the presence of EDCI, HOBT, and DIPEA at room temperature to provide the corresponding amide **17**. Cyclization of **17** by treatment with NaNO₂ in AcOH furnished the desired CRBN binders **18**. In the case of the CRBN binder **20** bearing carboxylic acid linkage, **18b** was treated with the corresponding amines, that is, glycine *tert*-butyl ester, azetidine carboxylic *tert*-butyl ester, and piperidine carboxylic *tert*-butyl ester in the presence of DIPEA in DMF to furnish intermediate **19**. The *tert*-butyl ester of **19** was converted to carboxylic acid **20** by treatment with 50% trifluoroacetic acid (TFA) in DCM. For the glycolic acid linkage **26**, intermediate **24** was prepared from hydroxynitrobenzoic acid **21** using a similar protocol with **18**. Then, **24** was treated with *tert*-butyl-2-bromoacetate in DMF at room temperature to provide **25**, which was converted to carboxylic acid **26** by TFA treatment.

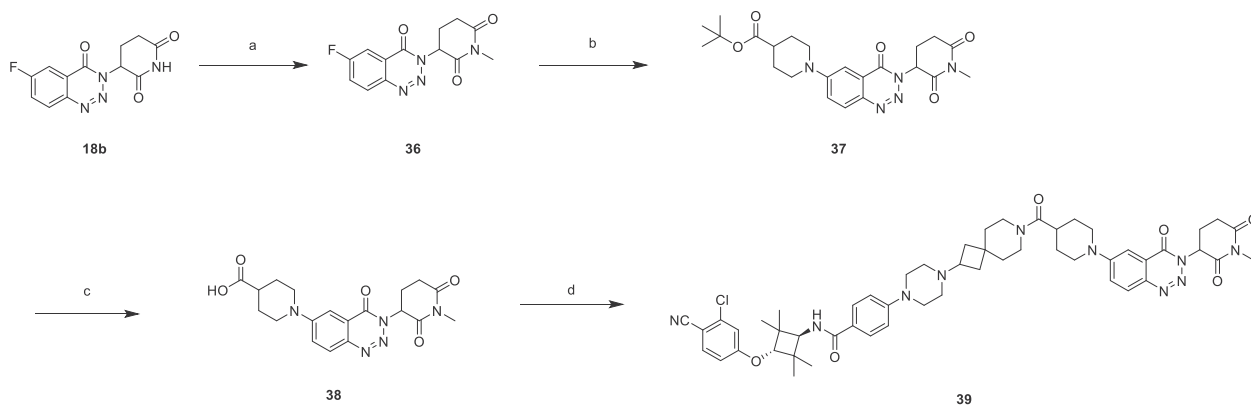
The synthesis of the AR PROTAC degraders is depicted in **Scheme 3**. We selected piperidine-based linkers of different lengths because the cyclic linker decreases the flexibility of large chimeric molecules, providing better physio-chemical properties, including the number of single rotational bonds. Reductive alkylation of **15** with

N-Boc-piperidine carboxaldehyde, *N*-Boc-2-oxo-7-azaspiro [3.5] nonane, or *tert*-butyl 4-(2-oxoethyl)piperidine-1-carboxylate provided the corresponding **27a**, **27b**, and **27c**, respectively. Alkylation of **15** with *tert*-butyl 4-(2-iodoethoxy)piperidine-1-carboxylate in the presence of K₂CO₃ at room temperature provided the corresponding **27d**. Following treatment with HCl, compounds of **27** were converted to **28**. Finally, conjugation with CRBN binders **18**, **20**, and **26** provided the corresponding degraders **29–35**, respectively, via either nucleophilic substitution reaction or treatment with EDCI, HOBT, and DIPEA in DMF. Compound **39** was synthesized as shown in **Scheme 4**. CRBN binder **18b** was treated with MeI in the presence of K₂CO₃ in DMF at room temperature to provide **36**. Substitution reaction with *tert*-butyl piperidine-4-carboxylate hydrochloride in the presence of DIPEA in DMF furnished intermediate **37**, which was converted to carboxylic acid **38** by treatment with 50% TFA in DCM. Conjugation with **28b** and **38** by treatment with EDCI, HOBT, and DIPEA in DMF provided **39**.

2.2. Evaluation of AR PROTACs

All compounds synthesized in this study were evaluated by





Scheme 4. Reagents and conditions: (a) MeI, K_2CO_3 , DMF, room temperature (rt); (b) *tert*-butyl piperidine-4-carboxylate hydrochloride, DIPEA, DMF, 90 °C; (c) TFA:DCM (1:1), room temperature; (d) **28b**, EDCI, HOBt, DIPEA, DMF, room temperature.

western blotting for AR degradation at three concentrations (0.1, 1, and 10 μ M). To examine the effects of the degraders, the anti-proliferative activity of degraders was tested in AR-dependent prostate cancer cell lines, LNCaP and VCaP. First, we investigated the linkage position in TD-106 (Table 1). Three compounds of **29** (for the 5-position) and four compounds of **30** (for the 6-position) were evaluated for AR degradation. Compound **29a**, attached to methylpiperidine at the 5-position, showed moderate AR degradation by 77% at 1 μ M, whereas **29b** and **29c**, attached with spirobutylpiperidine and ethylpiperazine in the 5-position, demonstrated weak AR degradation by 26% and 31% at 1 μ M, respectively. For the 6-position attachment, the methylpiperazine linker **30a** and ethoxyxypiperidine linker **30d** effectively reduced the AR level by 79% and 81% at 0.1 μ M, respectively. Compounds **30b** and **30c**, attached to the spirobutylpiperidine and ethylpiperidine linker, reduced the AR protein by 15% and 51% at 0.1 μ M, respectively; thus, these were less potent than **30a** and **30d**. In the

case of the 7-position with the methylpiperazine linker, **31a** demonstrated poor AR degradation by 28% at 0.1 μ M. It was observed that the linker conjugated to the 6-position of TD-106 (**30**) effectively reduced the AR protein level compared with linkers conjugated at the 5- and 7-positions (**29** and **31a**). Next, we evaluated the anti-proliferative activity of degraders in both LNCaP and VCaP prostate cancer cell lines. Compound **30** showed a better anti-proliferative effect in both cell lines than compound **29**. Overall, linker conjugation to the 6-position of TD-106 was superior to conjugation to the 5- and 7-positions for both AR degradation and anti-proliferative effects. In this study, VCaP cells were generally more sensitive than LNCaP cells to AR degraders.

Reportedly, the linker type and length of PRTOAC are critical for effective and targeted protein degradation [28,29]. Therefore, we further explored the linkers with different types of linkages with the CRBN ligand. Here, we selected four linkages, glycine (X1), azetidine carboxylic acid (X2), piperidine carboxylic acid (X3), and

Table 1
Investigation of linker attachment to TD-106 CRBN binder.

No.	CRBN binder	Linkers (AR \longleftrightarrow CRBN)	AR degradation in LNCaP(%)			Cytotoxicity(CC ₅₀ , μ M)	
			0.1 μ M	1 μ M	10 μ M	LNCaP	VCaP
29a			15	77	78	0.613	N.D.
29b			0	26	71	13.4	N.D.
29c			0	31	90	>10.0	1.58
30a			79	91	95	0.259	0.081
30b			15	95	81	0.214	0.113
30c			51	94	N.D.	0.449	0.120
30d			86	89	87	0.523	0.022
31a			28	60	83	N.D.	N.D.

glycolic acid (X4). We postulated that these linkages could affect the conformation of PROTAC or pharmacological properties, thereby providing superior molecules for *in vivo* studies. Using a combinatorial matrix approach, a total of 16 degraders were synthesized and evaluated for their potency in western blotting and anti-proliferative assays, as described in Table 2. In western blotting analyses, most compounds in this series effectively induced AR degradation by >60% at 0.1 μM , except for **33b**, **34a**, and **34d**. The anti-proliferative activity of AR PROTACs was evaluated in both LNCaP and VCaP cells. Degraders **32b**, **32c**, and **33c** demonstrated good anti-proliferative activities against both cell lines.

Next, we investigated the mechanism of AR degradation with the representative degrader **33c** (TD-802). A dose-dependent experiment was conducted to determine the DC_{50} and the maximum degradation (D_{max}) values, documented as 12.5 nM and 93%, respectively (Fig. 4A and B). Once androgen binds to the ligand-binding domain (LBD) of AR, the AR-androgen dimer regulates the transcription of its target genes. Some splice variants, including AR-V7, lacking the LBD are major androgen-independent drivers of AR-regulated gene expression in prostate cancer [30]. To determine if AR degraders can degrade endogenously expressed splice variant AR, TD-802 was treated in 22RV1 cells expressing both full-length AR and the AR-V7 splice variant. Western blotting analysis showed that TD-802 induced full-length AR protein degradation, with a D_{max} of 85% at 1 μM , but weak AR-V7 protein degradation with a D_{max} of 34% at 10 μM (Fig. 4C). To ascertain whether AR degradation by TD-802 is dependent on the ubiquitin-proteasome system and Cullin-Ring ubiquitin ligase, we examined the effects of bortezomib, the proteasome inhibitor, and MLN4924, the neddylation inhibitor, along with TD-802. Pretreatment with either bortezomib or MLN4924 completely inhibited TD-802-

Table 3
Stability of AR PROTACs in mouse liver microsomes.

Compound	% of remaining after 30 min ^a
30a	71.7 \pm 1.37
30c	86.7 \pm 1.28
30d	86.8 \pm 4.10
32b	92.8 \pm 0.41
32c	74.3 \pm 3.50
33a	85.5 \pm 0.41
33c	96.0 \pm 6.86
33d	62.8 \pm 3.77
34a	0.560 \pm 0.01
34b	92.9 \pm 2.80
34c	93.7 \pm 3.42
34d	2.98 \pm 0.08
35a	31.2 \pm 0.99
35b	92.6 \pm 2.20
35c	78.4 \pm 2.70
Buspiron (positive control)	0.03 \pm 0.01

^a Mean \pm SD, n = 3.

induced AR degradation (Fig. 4D). Time-course experiments indicated that TD-802 decreased AR levels by 80% after 4 h of incubation at 1 μM (Fig. 4E). However, **39** (TD-802-N-Me), which supposedly does not bind to CRBN, did not induce AR degradation (Fig. 4F) and exhibited a more 10-fold higher inhibition of proliferation than TD-802 in LNCaP (CC_{50} = 1.6 μM) and VCaP (CC_{50} = 0.499 μM) cell lines. These data indicate that the binding of TD-802 to CRBN is required for AR degradation and cell growth inhibitory activity.

Table 2
Study of linkage effect for androgen receptor (AR) degradation and anti-proliferative activity.

No.	Linker	X	AR degradation in LNCaP (%)			Anti-proliferative activity (CC_{50} , μM)	
			0.1 μM	1 μM	10 μM	LNCaP	VCaP
32a	L1	X1	70	89	35	0.117	3.82
32b		X2	96	96	83	0.089	0.038
32c		X3	90	89	94	0.108	0.045
32d		X4	89	40	51	0.804	N.C.
33a	L2	X1	61	77	39	0.208	0.054
33b		X2	0	79	0	0.312	0.135
33c		X3	85	93	95	0.098	0.044
33d		X4	60	77	79	0.196	0.076
34a	L3	X1	7	87	83	1.09	0.107
34b		X2	74	84	96	0.538	0.037
34c		X3	77	93	99	0.316	0.052
34d		X4	0	50	82	3.18	0.046
35a	L4	X1	77	95	88	0.852	0.057
35b		X2	82	86	90	0.762	0.057
35c		X3	72	92	98	0.847	0.080
35d		X4	86	98	94	1.30	0.141

N.C., not calculated.

Table 4
Pharmacokinetic parameters in male mice.

Compound	Injection	T _{max} (h)	C _{max} (µg/mL)	T _{1/2} (h)	AUC _t (µg·h/L)
30d	IV (5 mpk)	N/A	N/A	4.68	14.3
	IP (5 mpk)	2.0	1.78	4.51	10.7
	PO (30 mpk)	2.0	0.28	5.58	2.84
32b	IV (5 mpk)	N/A	N/A	4.48	24.1
	IP (5 mpk)	2.0	5.54	4.82	24.2
	PO (30 mpk)	0.67	0.05	26.7	0.44
33c	IV (5 mpk)	N/A	N/A	8.28	20.7
	IP (5 mpk)	0.03	2.78	4.41	1.72
	PO (30 mpk)	4.0	0.11	N/C	0.53
35b	IV (5 mpk)	N/A	N/A	4.35	4.49
	IP (5 mpk)	1.67	2.01	4.24	7.49
	PO (30 mpk)	0.7	0.02	19.7	0.15

N/A, not applicable; N/C, not calculated; IV, intravenous; IP, intraperitoneal; PO, peroral.

2.3. Pharmacokinetic studies of AR PROTACs

Based on the explicit effect of degraders in cells, we examined whether degraders possessed appropriate liver microsomal stability. Fifteen AR PROTACs were tested against mouse liver microsomes (Table 3). Most degraders were well-tolerated in the mouse liver microsomes, whereas three degraders, **34a**, **34d**, and **35a**, were quickly metabolized with less than 30% remaining after a 30-min incubation. A structure-microsomal stability relationship was not observed with the linker in this series.

To ensure that the microsomal studies accurately predict *in vivo* clearance, we assessed the *in vivo* pharmacokinetic (PK) properties of a single dose. Four representative compounds (**30d**, **32b**, **33c**, and **35b**) were selected and administered intravenously (IV), intraperitoneally (IP), and orally in this study (Fig. 5 and Table 4). The IV

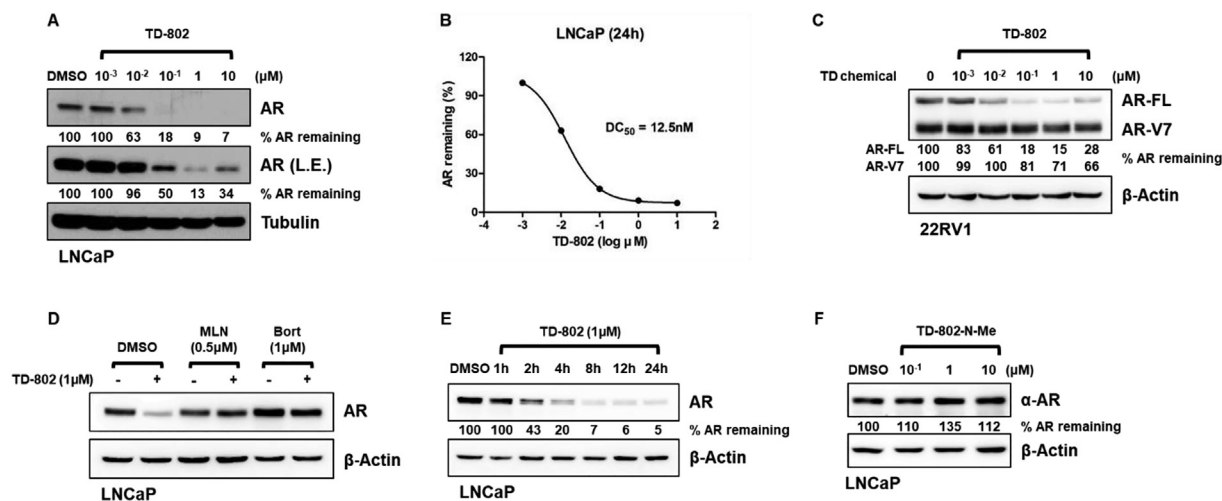


Fig. 4. Characterization of androgen receptor (AR) degradation by **33c** (TD-802). (A) A dose-dependent degradation of AR by TD-802. (B) Quantification of AR protein remaining and DC₅₀ graph from western blotting. (C) Degradation of full-length AR (AR-FL) and splicing variant (AR-V7) in 22RV1 cells. (D) UPS- and CRL-dependent AR degradation by TD-802. (E) Time-dependent AR degradation by TD-802. (F) Degradation of AR by **39** (TD-802-N-Me). DC₅₀, degradation concentration 50%; UPS, ubiquitin-proteasome system; CRL, Cullin-Ring ubiquitin ligase.

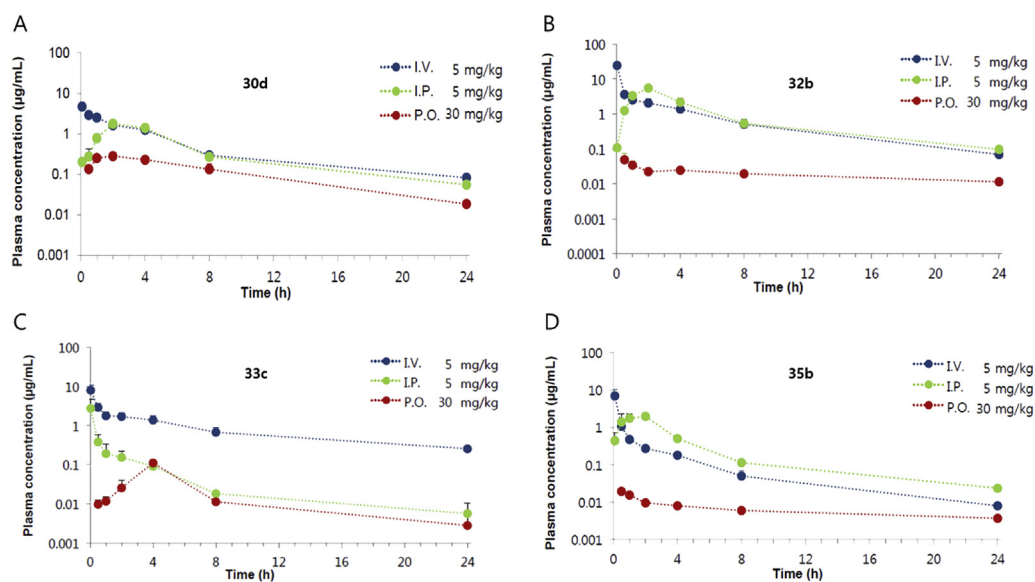


Fig. 5. Plasma concentration-time profiles in male mice (n = 3).

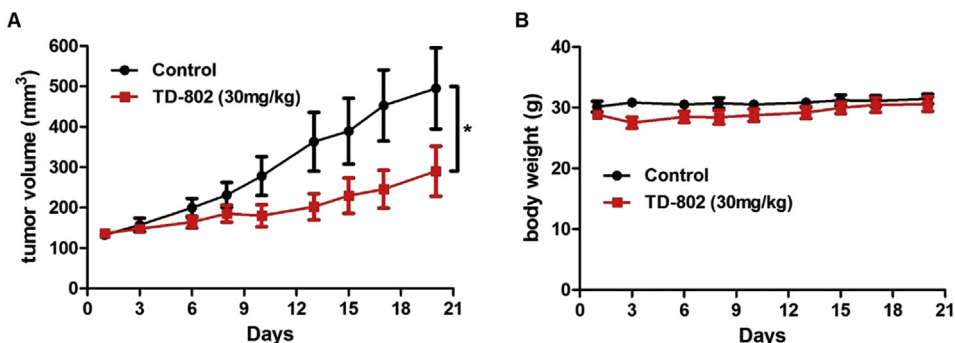


Fig. 6. Effect of TD-802 on tumor growth (A) and body weight (B) of VCaP prostate cancer in SCID mice. * $P = 0.0440$ vs. control group on the final day using Student's t-test.

half-life of all compounds was longer than 4 h; in particular, **33c** showed a considerably longer half-life ($t_{1/2} = 8.28$ h), which reflected a high plasma exposure ($AUC_t = 20.7 \mu\text{g h/L}$). In the case of IP administration, all compounds demonstrated similar half-lives of 4–5 h. Interestingly, **32b** exhibited the highest C_{max} value of $5.54 \mu\text{g/mL}$, which also reflected a high plasma exposure ($AUC_t = 24.2 \mu\text{g h/L}$); others demonstrated modest values of 1.78 – $2.78 \mu\text{g h/L}$. Notably, **33c** was quickly absorbed within 10 min after IP injection. Unfortunately, all degraders displayed extremely poor absorption after oral injection.

2.4. In vivo studies of 33c (TD-802)

To validate the antitumor activity of TD-802 *in vivo*, SCID mice (C-B-17/lcrCrj-scid, male) were injected with AR-positive VCaP prostate cancer cells and grown until the tumor size could be measured ($\sim 130 \text{ mm}^3$). Then, vehicle (control, 20% PEG400 + 3% Tween 80 in PBS) or TD-802 were administered intraperitoneally once a day for 10 days. Tumor volume and body weight were measured every 1–3 days after compound administration. The tumor growth rate was lower in mice administered TD-802 than in those administered vehicle during drug treatment and the tumor exhibited slow re-growth after stopping TD-802 treatment (Fig. 6A). No additional loss in body weight or off-target effects was observed (Fig. 6B). Collectively, these data demonstrated that the AR degrader, TD-802, effectively inhibited the growth of AR-positive tumors.

3. Conclusion

The AR protein plays a key role in prostate cancer. Thus, the inhibition of AR signaling by blocking androgen synthesis (e.g., abiraterone) or ligand binding to the AR (e.g., enzalutamide and apalutamide) is a common strategy for treating prostate cancer. Most patients initially respond to these drugs but partially exhibit drug resistance by genetic alterations such as gene amplification or mutations. Given these mechanisms of resistance, degradation of the AR protein by PROTAC can be considered an alternative method for mCRPC treatment.

In this study, we designed and evaluated a series of CRBN-mediated AR PROTACs, in which a tetramethylcyclobutane-based AR antagonist was linked with TD-106 CRBN binder. Most AR PROTACs synthesized in this study reduced the AR protein levels in LNCaP cells. In particular, we examined the effect of the linker position in the CRBN binder, TD-106, and observed that the 6-position in TD-106 was better than the 5-position for AR degradation. The elongation of the linker by different linkages in TD-106 improved AR degradation as well as proliferative inhibition of LNCaP and VCaP cells. The metabolic stability of AR PROTACs was

evaluated in mouse liver microsomes and most degraders displayed good microsomal stability, with $>70\%$ remaining after 30 min incubation. Additionally, *in vivo* PK studies showed that AR PROTACs displayed not only a long half-life of >4 h but also high plasma exposure following both IV and IP injections. Finally, TD-802 induced AR degradation demonstrated good antitumor efficacy in an *in vivo* xenograft mouse model, suggesting that CRBN-based AR degraders might be used for developing novel AR interventions. Further optimization efforts are currently under investigation for an orally bioavailable AR PROTAC degrader.

4. Experimental section

4.1. Chemistry

All reagents were obtained from commercial vendors and used without further purification. Thin layer chromatography was monitored by using pre-coated silica gel plates (Merck, art. 5715). Purification of all compounds was achieved by normal phase chromatographic technique (Silica gel 230–400 mesh). ^1H NMR and ^{13}C NMR were denoted in parts per million (ppm) and were recorded in Bruker Avance 300 and 500 using CDCl_3 , D_2O , CD_3OD , and $\text{DMSO}-d_6$. LC/MS analysis was executed with electron spray ionization technique with Agilent Technology 6130 quadrupole instrument.

4.1.1. Synthesis of tert-butyl 4-(4-(ethoxycarbonyl)phenyl)piperazine-1-carboxylate (**11**)

To a solution of ethyl 4-fluorobenzoate (5.0 g, 29.7 mmol) and tert-butyl piperazine-1-carboxylate (6.7 g, 35.64 mmol) in DMSO (40 mL) was added DIPEA (15.5 mL, 89.1 mmol). The mixture was stirred at 130°C for 24 h. The reaction mixture was cooled to room temperature and diluted with water and extracted with ethyl acetate. The organic layer was washed with brine, dried over Na_2SO_4 , and concentrated under reduced pressure. The residue was purified by column chromatography to afford **11** (5.5 g, 55%) as a white solid. ^1H NMR (300 MHz, CDCl_3) δ 7.97–7.88 (m, 2H), 6.89–6.82 (m, 2H), 4.33 (q, $J = 7.1$ Hz, 2H), 3.58 (m, 4H), 3.30 (m, 4H), 1.49 (s, 9H), 1.37 (t, $J = 7.1$ Hz, 3H).

4.1.2. Synthesis of 4-(4-(2-(1-(tert-butoxycarbonyl)piperidin-4-yl)ethyl)piperazin-1-yl)benzoic acid (**12**)

To a solution of **11** (5.5 g, 16.44 mmol) in MeOH (10 mL), H_2O (10 mL) and THF (40 mL) was added $\text{LiOH}\cdot\text{H}_2\text{O}$ (1 g, 24.66 mmol). The mixture was stirred at 40°C for 12 h. The reaction mixture was cooled to room temperature and concentrated. The crude residue was diluted with water and extracted with ethyl acetate. The aqueous layer was acidified with 1 N HCl solution, and the precipitate was washed with water and dried to afford **12** (1.6 g, 85%)

as a white solid. $^1\text{H NMR}$ (500 MHz, CDCl_3) δ 8.20–7.68 (m, 2H), 7.02–6.73 (m, 2H), 3.59 (t, $J = 5.2$ Hz, 4H), 3.34 (t, $J = 5.2$ Hz, 4H), 1.49 (s, 9H).

4.1.3. Synthesis of 4-((1R, 3R)-3-amino-2,2,4,4-tetramethylcyclobutoxy)-2-chlorobenzonitrile hydrogen chloride (**13**)

Compound **13** was prepared by a similar procedure reported in the literature [26]. $^1\text{H NMR}$ (400 MHz, D_2O) δ 7.74 (d, $J = 8.8$ Hz, 1H), 7.19 (d, $J = 2.4$ Hz, 1H), 7.00 (dd, $J = 8.8, 2.5$ Hz, 1H), 4.42 (s, 1H), 3.36 (s, 1H), 1.37 (s, 6H), 1.19 (s, 6H).

4.1.4. Synthesis of tert-butyl 4-(4-(((1R,3R)-3-(3-chloro-4-cyanophenoxy)-2,2,4,4-tetramethylcyclobutyl) carbamoyl)phenyl) piperazine-1-carboxylate (**14**)

To a solution of **12** (1.5 g, 4.75 mmol), **13** (2.9 g, 9.51 mmol), $\text{EDCI}\cdot\text{HCl}$ (1.0 g, 5.22 mmol), and HOBT (0.705 g, 5.22 mmol) in DMF (20 mL) was added DIPEA (3.3 mL, 19.0 mmol). The mixture was stirred at room temperature for 12 h. The reaction mixture was diluted with water and extracted with ethyl acetate. The organic layer was washed with brine, dried over Na_2SO_4 , and concentrated under reduced pressure. The residue was purified by column chromatography to afford **14** (2.2 g, 81%) as a white solid. $^1\text{H NMR}$ (300 MHz, CDCl_3) δ 7.78–7.64 (m, 2H), 7.57 (d, $J = 8.7$ Hz, 1H), 6.97 (d, $J = 2.4$ Hz, 1H), 6.94–6.89 (m, 2H), 6.81 (dd, $J = 8.7, 2.5$ Hz, 1H), 6.14 (d, $J = 8.1$ Hz, 1H), 4.15 (d, $J = 9.0$ Hz, 1H), 4.05 (s, 1H), 3.65–3.56 (m, 4H), 3.27 (m, 4H), 1.49 (s, 9H), 1.27 (s, 6H), 1.22 (s, 6H).

4.1.5. Synthesis of N-(((1R,3R)-3-(3-chloro-4-cyanophenoxy)-2,2,4,4-tetramethylcyclobutyl)-4-(piperazin-1-yl) benzamide (**15**)

To a solution of **14** (1.5 g, 2.64 mmol) in DCM (10 mL) was added 4.0 N HCl in dioxane (1.0 mL). The mixture was stirred at room temperature for 3 h and concentrated under reduced pressure. The crude residue was diluted with 5% K_2CO_3 and extracted with ethyl acetate. The organic layer was washed with brine, dried over Na_2SO_4 , and concentrated under reduced pressure. The residue was purified by column chromatography to afford **15** (1.0 g, 83%) as a white solid. $^1\text{H NMR}$ (300 MHz, CDCl_3) δ 7.70 (m, 2H), 7.57 (d, $J = 8.7$ Hz, 1H), 6.97 (d, $J = 2.4$ Hz, 1H), 6.94–6.88 (m, 2H), 6.81 (dd, $J = 8.7, 2.4$ Hz, 1H), 6.11 (d, $J = 8.2$ Hz, 1H), 4.15 (d, $J = 8.1$ Hz, 1H), 4.04 (s, 1H), 3.40–3.19 (m, 4H), 3.13–2.97 (m, 4H), 1.26 (m, 7H), 1.22 (s, 6H).

4.1.6. Synthesis of 2-amino-N-(2,6-dioxopiperidin-3-yl)-6-fluorobenzamide (**17a**)

To a solution of 2-amino-6-fluoro-benzoic acid (5 g, 32.23 mmol), 3-amino pyridine-2,6-dione hydrochloride (5.26 g, 35.45 mmol), $\text{EDCI}\cdot\text{HCl}$ (6.8 g, 35.45 mmol), and HOBT (4.8 g, 35.45 mmol) in DMF (150 mL) was added DIPEA (17 mL, 96.69 mmol). The mixture was stirred at room temperature for 12 h. The reaction mixture was diluted with water and extracted with ethyl acetate. The organic layer was washed with brine, dried over Na_2SO_4 and concentrated under reduced pressure. The crude compound **17a** was obtained as a yellow solid (8.0 g, 94%) and used in the next step without further purification. $^1\text{H NMR}$ (300 MHz, $\text{DMSO}-d_6$) δ 10.90 (s, 1H), 8.53 (dd, $J = 8.2, 2.8$ Hz, 1H), 7.10 (m, 1H), 6.52 (d, $J = 8.2$ Hz, 1H), 6.33 (dd, $J = 10.6, 8.1$ Hz, 1H), 6.00 (s, 2H), 4.75 (m, 1H), 2.88–2.69 (m, 1H), 2.57 (m, 1H), 2.20–1.94 (m, 2H).

4.1.7. Synthesis of N-(2,6-dioxopiperidin-3-yl)-5-fluoro-2-nitrobenzamide (**17b**)

Similar procedure of **17a** was performed to give **17b** (5 g, 58%) as a grey solid. $^1\text{H NMR}$ (500 MHz, $\text{DMSO}-d_6$) δ 10.86 (s, 1H), 8.55 (d, $J = 8.3$ Hz, 1H), 7.37 (dd, $J = 10.5, 3.0$ Hz, 1H), 7.08 (m, 1H), 6.73 (dd, $J = 9.1, 4.9$ Hz, 1H), 6.33 (s, 2H), 4.73 (m, 1H), 2.84–2.71 (m, 1H), 2.55

(m, 1H), 2.09 (m, 1H), 2.00–1.89 (m, 1H).

4.1.8. Synthesis of 2-amino-N-(2,6-dioxopiperidin-3-yl)-4-fluorobenzamide (**17c**)

Similar procedure of **17a** was performed to give **17c** (240 mg, 71%) as white solid. $^1\text{H NMR}$ (500 MHz, $\text{DMSO}-d_6$) δ 10.85 (s, 1H), 8.50 (d, $J = 8.4$ Hz, 1H), 7.64–7.54 (m, 1H), 6.77 (s, 2H), 6.48 (d, $J = 11.1$ Hz, 1H), 6.36 (t, $J = 8.3$ Hz, 1H), 4.72 (m, 1H), 2.84–2.73 (m, 1H), 2.56 (m, 1H), 2.18–2.06 (m, 1H), 1.96 (m, 1H).

4.1.9. Synthesis of 3-(5-fluoro-4-oxobenzo[d][1,2,3] triazin-3(4H)-yl)piperidine-2,6-dione (**18a**)

To a solution of **17a** (5 g, 56.55 mmol) in AcOH (120 mL) was added sodium nitrite (2.2 g, 32.04 mmol). The mixture was stirred at room temperature for 2 h. The mixture was diluted with water and the white precipitate was collected, washed with water, dried to afford **18a** (4 g, 75%). $^1\text{H NMR}$ (300 MHz, $\text{DMSO}-d_6$) δ 11.21 (s, 1H), 8.24–8.03 (m, 2H), 7.86–7.72 (m, 1H), 5.97 (dd, $J = 12.1, 5.4$ Hz, 1H), 2.96 (m, 1H), 2.76–2.58 (m, 2H), 2.35–2.16 (m, 1H).

4.1.10. Synthesis of 3-(6-fluoro-4-oxobenzo[d][1,2,3] triazin-3(4H)-yl)piperidine-2,6-dione (**18b**)

Similar procedure of **18a** was performed to give **18b** (4.8 g, 88%) as a yellow solid. $^1\text{H NMR}$ (400 MHz, $\text{DMSO}-d_6$) δ 11.21 (s, 1H), 8.46–8.34 (m, 1H), 8.04 (m, 2H), 6.00 (dd, $J = 12.4, 5.4$ Hz, 1H), 3.05–2.90 (m, 1H), 2.81–2.62 (m, 2H), 2.39–2.21 (m, 1H).

4.1.11. Synthesis of 3-(7-fluoro-4-oxobenzo[d][1,2,3] triazin-3(4H)-yl)piperidine-2,6-dione (**18c**)

Similar procedure of **18a** was performed to give **18c** (200 mg, 80%) as white solid. $^1\text{H NMR}$ (300 MHz, $\text{DMSO}-d_6$) δ 11.22 (s, 1H), 8.37 (dd, $J = 8.8, 5.6$ Hz, 1H), 8.17 (dd, $J = 8.9, 2.5$ Hz, 1H), 7.87 (m, 1H), 6.01 (dd, $J = 12.2, 5.4$ Hz, 1H), 3.08–2.89 (m, 1H), 2.81–2.57 (m, 2H), 2.30 (m, 1H).

4.1.12. Synthesis of tert-butyl (3-(2,6-dioxopiperidin-3-yl)-4-oxo-3,4-dihydrobenzo[d][1,2,3] triazin-6-yl)glycinate (**19a**)

To a solution of **18b** (1 g, 3.6 mmol) and glycine tert-butyl ester hydrochloride (902 mg, 5.4 mmol) in DMSO (20 mL) was added DIPEA (2.5 mL, 14.4 mmol). The reaction mixture was stirred at 90 °C for 2 h. The mixture was diluted with water and the white precipitate was collected, washed with water, dried to afford **19a**. $^1\text{H NMR}$ (300 MHz, CDCl_3) δ 8.12 (s, 1H), 7.95 (m, 1H), 7.17 (m, 2H), 5.79 (dd, $J = 11.5, 5.1$ Hz, 1H), 5.24 (m, 1H), 3.94 (d, $J = 4.8$ Hz, 2H), 3.08–2.76 (m, 3H), 2.44–2.32 (m, 1H), 1.52 (s, 9H).

4.1.13. Synthesis of tert-butyl 1-(3-(2,6-dioxopiperidin-3-yl)-4-oxo-3,4-dihydrobenzo[d][1,2,3] triazin-6-yl)azetidine-3-carboxylate (**19b**)

Similar procedure of **19a** was performed to give **19b** (800 mg, 53%) as a white solid. $^1\text{H NMR}$ (500 MHz, CDCl_3) δ 8.07 (s, 1H), 7.98 (dd, $J = 8.9, 1.4$ Hz, 1H), 7.06 (m, 1H), 6.93 (m, 1H), 5.77 (dd, $J = 11.4, 5.4$ Hz, 1H), 4.26 (t, $J = 8.4$ Hz, 2H), 4.21 (t, $J = 7.0$ Hz, 2H), 3.59–3.51 (m, 1H), 3.01–2.81 (m, 3H), 2.38 (m, 1H), 1.49 (s, 9H).

4.1.14. Synthesis of tert-butyl 2-(1-(3-(2,6-dioxopiperidin-3-yl)-4-oxo-3,4-dihydrobenzo[d][1,2,3] triazin-6-yl)piperidin-4-yl)acetate (**19c**)

Similar procedure of **19a** was performed to give **19c** (850 mg, 53%) as a yellow solid. $^1\text{H NMR}$ (300 MHz, $\text{DMSO}-d_6$) δ 11.16 (s, 1H), 8.01 (d, $J = 9.2$ Hz, 1H), 7.72 (dd, $J = 9.3, 2.9$ Hz, 1H), 7.38 (d, $J = 2.8$ Hz, 1H), 5.89 (dd, $J = 12.3, 5.4$ Hz, 1H), 4.09–3.94 (m, 3H), 3.12 (t, $J = 12.2$ Hz, 2H), 3.02–2.88 (m, 1H), 2.76–2.60 (m, 2H), 2.23 (m, 1H), 1.91 (d, $J = 13.2$ Hz, 2H), 1.61 (m, 2H), 1.41 (s, 9H).

4.1.15. Synthesis of (3-(2,6-dioxopiperidin-3-yl)-4-oxo-3,4-dihydrobenzo[d][1,2,3] triazin-6-yl)glycine (**20a**)

To a solution of **19a** (1.0 g, 2.5 mmol) in DCM (15 mL) was added TFA (15 mL). The reaction mixture was stirred at room temperature for 1 h and concentrated. The crude residue was purified by silica gel chromatography to afford **20a** (600 mg, 70%) as a white solid. ¹H NMR (300 MHz, DMSO-*d*₆) δ 12.84 (s, 1H), 11.14 (s, 1H), 7.94 (d, *J* = 8.9 Hz, 1H), 7.50 (t, *J* = 6.0 Hz, 1H), 7.38 (dd, *J* = 8.9, 2.6 Hz, 1H), 7.11–6.97 (m, 1H), 5.86 (dd, *J* = 12.2, 5.4 Hz, 1H), 4.06 (d, *J* = 5.9 Hz, 2H), 2.96 (m, 1H), 2.66 (m, 2H), 2.23 (m, 1H).

4.1.16. Synthesis of 1-(3-(2,6-dioxopiperidin-3-yl)-4-oxo-3,4-dihydrobenzo[d][1,2,3] triazin-6-yl)azetidine-3-carboxylic acid (**20b**)

Similar procedure of **20a** was performed to give **20b** (512 mg, 76%) as a white solid. ¹H NMR (300 MHz, DMSO-*d*₆) δ 12.79 (s, 1H), 11.14 (s, 1H), 8.01 (d, *J* = 8.9 Hz, 1H), 7.15 (dd, *J* = 8.9, 2.6 Hz, 1H), 6.91 (d, *J* = 2.6 Hz, 1H), 5.88 (dd, *J* = 12.2, 5.4 Hz, 1H), 4.28 (t, *J* = 8.6 Hz, 2H), 4.15 (m, 2H), 3.72–3.55 (m, 1H), 2.96 (m, 1H), 2.76–2.59 (m, 2H), 2.29–2.16 (m, 1H).

4.1.17. Synthesis of 1-(3-(2,6-dioxopiperidin-3-yl)-4-oxo-3,4-dihydrobenzo[d][1,2,3] triazin-6-yl)piperidine-4-carboxylic acid (**20c**)

Similar procedure of **20a** was performed to give **20c** (500 mg, 67%) as a white solid. ¹H NMR (300 MHz, DMSO) δ 12.31 (s, 1H), 11.15 (s, 1H), 8.01 (d, *J* = 9.2 Hz, 1H), 7.72 (dd, *J* = 9.3, 2.9 Hz, 1H), 7.38 (d, *J* = 2.8 Hz, 1H), 5.89 (dd, *J* = 12.2, 5.4 Hz, 1H), 4.01 (d, *J* = 13.5 Hz, 2H), 3.20–3.06 (m, 2H), 3.01–2.88 (m, 1H), 2.76–2.56 (m, 3H), 2.24 (m, 1H), 1.98–1.86 (m, 2H), 1.62 (m, 2H).

4.1.18. Synthesis of *N*-(2,6-dioxopiperidin-3-yl)-5-hydroxy-2-nitrobenzamide (**22**)

To a solution of **21** (5 g, 27.3 mmol), 3-aminopiperidine-2,6-dione hydrochloride (3.5 g, 27.3 mmol), EDCI·HCl (5.8 g, 30.03 mmol), and HOBt (4 g, 30.03 mmol) in DMF (20 mL) was added DIPEA (19 mL, 109.2 mmol). The reaction mixture was stirred at room temperature for 12 h. The reaction mixture was diluted with water and extracted with ethyl acetate. The organic layer was washed with brine, dried over Na₂SO₄, and concentrated under reduced pressure. The residue was purified by column chromatography to afford **22** (7.5 g, 93%) as a yellow solid. ¹H NMR (500 MHz, CD₃OD) δ 7.98 (d, *J* = 8.7 Hz, 1H), 6.89–6.82 (m, 2H), 4.72 (dd, *J* = 12.6, 5.2 Hz, 1H), 2.79–2.69 (m, 1H), 2.67–2.57 (m, 1H), 2.29–2.16 (m, 1H), 2.01 (m, 1H).

4.1.19. Synthesis of 2-amino-*N*-(2,6-dioxopiperidin-3-yl)-5-hydroxybenzamide (**23**)

To a solution of **22** (7.5 g, 25.5 mmol) in MeOH (4 mL) was added 10% Pd/C (0.725 g). The reaction mixture was stirred at room temperature for 12 h under hydrogen gas environment. The solution was filtered through a pad of Celite and removed under vacuum to give crude oil. The crude residue was purified by silica gel column chromatography to afford **23** (2.5 g, 38%) as a blue solid. ¹H NMR (500 MHz, DMSO-*d*₆) δ 10.84 (s, 1H), 8.62 (s, 1H), 8.42 (d, *J* = 8.4 Hz, 1H), 6.93 (d, *J* = 2.8 Hz, 1H), 6.71 (dd, *J* = 8.7, 2.7 Hz, 1H), 6.57 (d, *J* = 8.7 Hz, 1H), 5.72 (s, 2H), 4.71 (m, 1H), 2.78, (m, 1H), 2.54 (m, 1H), 2.09 (m, 1H), 1.97–1.83 (m, 1H).

4.1.20. Synthesis of 3-(6-hydroxy-4-oxobenzo[d][1,2,3] triazin-3(4H)-yl)piperidine-2,6-dione (**24**)

To a solution of **23** (2.5 g, 9.1 mmol) in AcOH (120 mL) was added sodium nitrite (1.3 g, 18.2 mmol). The reaction mixture was stirred at room temperature for 2 h. The reaction mixture was diluted with water and extracted with ethyl acetate. The organic layer was

washed with brine, dried over Na₂SO₄, and concentrated under reduced pressure. The residue was purified by column chromatography to afford **24** (1 g, 40%) as an ivory solid. ¹H NMR (500 MHz, DMSO-*d*₆) δ 11.18 (s, 1H), 8.13 (d, *J* = 8.8 Hz, 1H), 7.51 (dd, *J* = 8.9, 2.7 Hz, 1H), 7.47 (d, *J* = 2.6 Hz, 1H), 5.92 (dd, *J* = 12.5, 5.4 Hz, 1H), 3.05–2.88 (m, 1H), 2.73–2.59 (m, 2H), 2.25 (m, 1H).

4.1.21. Synthesis of *tert*-butyl 2-((3-(2,6-dioxopiperidin-3-yl)-4-oxo-3,4-dihydrobenzo[d][1,2,3] triazin-6-yl)oxy)acetate (**25**)

To a solution of **24** (1 g, 3.64 mmol) and potassium carbonate (0.497 g, 3.6 mmol) in DMF (10 mL) was added *tert*-butyl bromoacetate (0.3 mL, 2.1 mmol). The reaction mixture was stirred at room temperature for 3 h. The reaction mixture was quenched with water and then extracted with ethyl acetate. The organic layer was washed with brine, dried over Na₂SO₄, and concentrated under reduced pressure. The residue was purified by column chromatography to afford **25** (1 g, 72%) as a white solid. ¹H NMR (500 MHz, DMSO-*d*₆) δ 11.22 (s, 1H), 8.23 (d, *J* = 9.0 Hz, 1H), 7.72 (dd, *J* = 9.0, 2.9 Hz, 1H), 7.53 (d, *J* = 2.9 Hz, 1H), 6.03–5.91 (m, 1H), 5.00 (s, 2H), 3.02–2.91 (m, 1H), 2.75–2.63 (m, 2H), 2.31–2.23 (m, 1H), 1.44 (s, 9H).

4.1.22. Synthesis of 2-((3-(2,6-dioxopiperidin-3-yl)-4-oxo-3,4-dihydrobenzo[d][1,2,3] triazin-6-yl)oxy)acetic acid (**26**)

To a solution of **25** (1.0 g, 2.5 mmol) in DCM (15 mL) was added TFA (15 mL). The reaction mixture was stirred at room temperature for 1 h. The reaction mixture was concentrated under vacuum to afford crude solid. The crude solid was purified by silica gel chromatography to afford **26** (625 mg, 79%) as a white solid. ¹H NMR (400 MHz, DMSO-*d*₆) δ 11.18 (s, 1H), 8.22 (d, *J* = 9.0 Hz, 1H), 7.72 (dd, *J* = 9.0, 2.9 Hz, 1H), 7.55 (d, *J* = 2.9 Hz, 1H), 6.01–5.90 (m, 1H), 5.01 (s, 2H), 3.04–2.90 (m, 1H), 2.78–2.62 (m, 2H), 2.32–2.22 (m, 1H).

4.1.23. Synthesis of *tert*-butyl 4-((4-(4-(((1*r*,3*r*)-3-(3-chloro-4-cyanophenoxy)-2,2,4,4-tetramethylcyclobutyl) carbamoyl) phenyl) piperazin-1-yl)methyl)piperidine-1-carboxylate (**27a**)

To a mixture of **15** (700 mg, 1.49 mmol), *tert*-butyl 4-formylpiperidine-1-carboxylate (1.3 g, 5.99 mmol), and AcOH (1.0 mL) in MeOH (15 mL) was added NaBH₃CN (561 mg, 8.94 mmol). The mixture was stirred at room temperature for 12 h. The reaction mixture was concentrated under reduced pressure. The residue was quenched with saturated NaHCO₃ solution and extracted with dichloromethane. The organic layer was washed with brine, dried over Na₂SO₄, and concentrated under reduced pressure. The residue was purified by column chromatography to afford **27a** (700 mg, 70%) as a white solid. ¹H NMR (400 MHz, CDCl₃) δ 7.73–7.65 (m, 2H), 7.56 (d, *J* = 8.7 Hz, 1H), 6.97 (d, *J* = 2.4 Hz, 1H), 6.94–6.89 (m, 2H), 6.81 (dd, *J* = 8.7, 2.4 Hz, 1H), 6.11 (d, *J* = 8.2 Hz, 1H), 4.14 (m, 2H), 4.04 (m, 2H), 3.29 (t, *J* = 5.0 Hz, 4H), 2.71 (t, *J* = 12.6 Hz, 2H), 2.56 (t, *J* = 5.1 Hz, 4H), 2.23 (d, *J* = 7.0 Hz, 2H), 1.75 (d, *J* = 13.5 Hz, 2H), 1.67 (m, 1H), 1.46 (s, 9H), 1.26 (s, 6H), 1.22 (s, 6H), 1.16–1.05 (m, 2H); LC/MS (M + H)⁺ (*m/z*) 664.1.

4.1.24. Synthesis of *tert*-butyl 2-(4-(4-(((1*r*,3*r*)-3-(3-chloro-4-cyanophenoxy)-2,2,4,4-tetramethylcyclobutyl) carbamoyl) phenyl) piperazin-1-yl)-7-azaspiro[3.5]nonane-7-carboxylate (**27b**)

Similar procedure of **27a** was performed to give **27b** (450 mg, 93%) as a white solid. ¹H NMR (500 MHz, CDCl₃) δ 7.69 (d, *J* = 8.4 Hz, 2H), 7.57 (d, *J* = 8.7 Hz, 1H), 6.96 (t, *J* = 1.8 Hz, 1H), 6.91 (d, *J* = 8.5 Hz, 2H), 6.83–6.75 (m, 1H), 6.10 (d, *J* = 8.1 Hz, 1H), 4.15 (d, *J* = 8.0 Hz, 1H), 4.04 (s, 1H), 3.37 (m, 2H), 3.30 (m, 6H), 2.74 (p, *J* = 7.9 Hz, 1H), 2.47 (t, *J* = 5.0 Hz, 4H), 2.05 (t, *J* = 9.5 Hz, 2H), 1.67 (t, *J* = 9.6 Hz, 2H), 1.58 (m, 2H), 1.51 (t, *J* = 5.7 Hz, 2H), 1.45 (s, 9H), 1.26 (s, 6H), 1.22 (s, 6H); LC/MS (M + H)⁺ (*m/z*) 690.2.

4.1.25. Synthesis of *tert*-butyl 4-(2-(4-(4-(((1*R*,3*R*)-3-(3-chloro-4-cyanophenoxy)-2,2,4,4-tetramethylcyclobutyl) carbamoyl) phenyl) piperazin-1-yl)ethyl)piperidine-1-carboxylate (**27c**)

Similar procedure of **27a** was performed to give **27c** (400 mg, 92%) as a white solid. ¹H NMR (500 MHz, CDCl₃) δ 7.69 (d, *J* = 8.6 Hz, 2H), 7.56 (d, *J* = 8.7 Hz, 1H), 6.96 (d, *J* = 2.4 Hz, 1H), 6.91 (d, *J* = 8.9 Hz, 2H), 6.81 (dd, *J* = 8.7, 2.4 Hz, 1H), 6.13 (d, *J* = 8.1 Hz, 1H), 4.15 (d, *J* = 8.1 Hz, 1H), 4.05 (s, 1H), 3.37 (t, *J* = 4.9 Hz, 4H), 2.71 (m, 6H), 2.53 (t, *J* = 7.8 Hz, 3H), 1.67 (d, *J* = 12.6 Hz, 2H), 1.57–1.49 (m, 2H), 1.46 (s, 9H), 1.26 (m, 8H), 1.22 (s, 6H), 1.13 (m, 2H); LC/MS (M + H)⁺ (*m/z*) 678.47.

4.1.26. Synthesis of *tert*-butyl 4-(2-(4-(4-(((1*R*,3*R*)-3-(3-chloro-4-cyanophenoxy)-2,2,4,4-tetramethylcyclobutyl) carbamoyl) phenyl) piperazin-1-yl)ethoxy)piperidine-1-carboxylate (**27d**)

To a solution of **13** (700 mg, 1.49 mmol) and potassium carbonate (412 mg, 2.98 mmol) in DMF (20 mL) was added *tert*-butyl 4-(2-iodoethoxy) piperidine-1-carboxylate (793 mg, 2.2 mmol). The mixture was stirred at room temperature overnight. The reaction was quenched with water and extracted with ethyl acetate. The organic layer was washed with brine, dried over Na₂SO₄ and concentrated under reduced pressure. The residue was purified by column chromatography to afford **27d** (820 mg, 70%) as a white solid. ¹H NMR (300 MHz, CDCl₃) δ 7.71 (d, *J* = 8.8 Hz, 2H), 7.58 (d, *J* = 8.7 Hz, 1H), 6.98 (d, *J* = 2.4 Hz, 1H), 6.93 (d, *J* = 8.8 Hz, 2H), 6.83 (dd, *J* = 8.7, 2.4 Hz, 1H), 6.13 (d, *J* = 8.1 Hz, 1H), 4.17 (d, *J* = 8.5 Hz, 1H), 4.06 (s, 1H), 3.88–3.72 (m, 2H), 3.67 (t, *J* = 5.8 Hz, 2H), 3.48 (m, 1H), 3.34 (t, *J* = 5.1 Hz, 4H), 3.11 (m, 2H), 2.70 (m, 6H), 1.93–1.78 (m, 2H), 1.56 (m, 2H), 1.48 (s, 9H), 1.28 (s, 6H), 1.24 (s, 6H).

4.1.27. Synthesis of *N*-(((1*R*,3*R*)-3-(3-chloro-4-cyanophenoxy)-2,2,4,4-tetramethylcyclobutyl)-4-(4-(piperidin-4-yl)methyl) piperazin-1-yl) benzamide hydrochloride (**28a**)

A mixture of **27a** (700 mg, 1.053 mmol) and 4.0 N HCl in dioxane (2 mL) in DCM (10 mL) was stirred at room temperature for 2 h. The mixture was concentrated under reduced pressure to afford **28a** (600 mg, 94%) as a white solid. ¹H NMR (500 MHz, CD₃OD) δ 7.81 (d, *J* = 8.3 Hz, 2H), 7.72 (d, *J* = 8.7 Hz, 1H), 7.16–7.05 (m, 3H), 6.98 (d, *J* = 8.8 Hz, 1H), 4.29 (s, 1H), 4.14 (s, 1H), 4.02 (d, *J* = 13.7 Hz, 2H), 3.76 (m, 2H), 3.65 (m, 3H), 3.46 (d, *J* = 13.1 Hz, 2H), 3.37 (t, *J* = 12.7 Hz, 2H), 3.23 (d, *J* = 6.8 Hz, 2H), 3.09 (t, *J* = 12.9 Hz, 2H), 2.15 (d, *J* = 14.5 Hz, 2H), 1.59 (q, *J* = 12.8 Hz, 2H), 1.28 (s, 6H), 1.22 (s, 6H); LC/MS (M + H)⁺ (*m/z*) 564.1.

4.1.28. Synthesis of 4-(4-(7-azaspiro [3.5] nonan-2-yl) piperazin-1-yl)-*N*-(((1*R*,3*R*)-3-(3-chloro-4-cyanophenoxy)-2,2,4,4-tetramethylcyclobutyl) benzamide hydrochloride (**28b**)

Similar procedure of **28a** was performed to give **28b** (350 mg, 90%) as a white solid. ¹H NMR (300 MHz, CD₃OD) δ 7.83 (d, *J* = 8.8 Hz, 2H), 7.74 (d, *J* = 8.8 Hz, 1H), 7.15 (d, *J* = 2.4 Hz, 1H), 7.12 (d, *J* = 8.8 Hz, 2H), 7.01 (dd, *J* = 8.8, 2.4 Hz, 1H), 4.32 (s, 1H), 4.16 (s, 1H), 4.07 (d, *J* = 13.7 Hz, 2H), 3.86 (t, *J* = 8.3 Hz, 1H), 3.78–3.58 (m, 3H), 3.22 (t, *J* = 5.7 Hz, 2H), 3.18–3.04 (m, 4H), 2.50–2.30 (m, 4H), 1.96 (q, *J* = 6.5 Hz, 4H), 1.87–1.74 (m, 1H), 1.30 (s, 6H), 1.24 (s, 6H); LC/MS (M + H)⁺ (*m/z*) 590.1.

4.1.29. Synthesis of 4-(4-(7-azaspiro [3.5] nonan-2-yl) piperazin-1-yl)-*N*-(((1*R*,3*R*)-3-(3-chloro-4-cyanophenoxy)-2,2,4,4-tetramethylcyclobutyl) benzamide hydrochloride (**28c**)

Similar procedure of **28a** was performed to give **28c** (330 mg, 90%) as a white solid. ¹H NMR (500 MHz, CD₃OD) δ 7.83 (d, *J* = 8.3 Hz, 2H), 7.74 (d, *J* = 8.7 Hz, 1H), 7.15 (m, 1H), 7.12 (d, *J* = 8.4 Hz, 2H), 7.01 (m, 1H), 4.32 (s, 1H), 4.17 (s, 1H), 4.07 (m, 2H), 3.79–3.66 (m, 3H), 3.44 (d, *J* = 12.9 Hz, 2H), 3.32–3.26 (m, 4H), 3.04 (t, *J* = 12.6 Hz, 2H), 2.04 (d, *J* = 14.0 Hz, 2H), 1.91–1.83 (m, 2H),

1.58–1.48 (m, 2H), 1.31 (m, 8H), 1.25 (s, 6H).

4.1.30. Synthesis of *N*-(((1*R*,3*R*)-3-(3-chloro-4-cyanophenoxy)-2,2,4,4-tetramethylcyclobutyl)-4-(4-(2-(piperidin-4-yloxy) ethyl) piperazin-1-yl) benzamide hydrochloride (**28d**)

Similar procedure of **28a** was performed to give **28d** (680 mg, 91%) as a white solid. ¹H NMR (300 MHz, DMSO-*d*₆) δ 11.43 (s, 1H), 9.09 (s, 2H), 7.91 (d, *J* = 8.7 Hz, 1H), 7.82 (d, *J* = 8.5 Hz, 2H), 7.64 (d, *J* = 9.2 Hz, 1H), 7.21 (d, *J* = 2.4 Hz, 1H), 7.05 (d, *J* = 8.7 Hz, 1H), 7.01 (dd, *J* = 8.8, 2.4 Hz, 1H), 4.35 (s, 1H), 4.07 (d, *J* = 9.2 Hz, 1H), 4.00–3.82 (m, 4H), 3.75–3.53 (m, 4H), 3.38 (m, 4H), 3.24 (m, 3H), 3.03–2.87 (m, 2H), 2.00 (m, 2H), 1.77 (m, 2H), 1.23 (s, 6H), 1.13 (s, 6H).

4.1.31. Synthesis of *N*-(((1*R*,3*R*)-3-(3-chloro-4-cyanophenoxy)-2,2,4,4-tetramethylcyclobutyl)-4-(4-(1-(3-(2,6-dioxopiperidin-3-yl)-4-oxo-3,4-dihydrobenzo[d][1,2,3]triazin-5-yl)piperidin-4-yl) methyl)piperazin-1-yl)benzamide (**29a**)

To a solution of **28a** (80 mg, 0.133 mmol) and **18a** (44 mg, 0.159 mmol) in DMF (10 mL) was added DIPEA (0.092 mL, 0.532 mmol). The reaction mixture was stirred at 90 °C for 12 h. The reaction mixture was diluted with water and extracted with ethyl acetate. The organic layer was washed with brine, dried over Na₂SO₄ and concentrated under reduced pressure. The residue was purified by column chromatography to afford **29a** (68 mg, 62%) as a yellow solid. ¹H NMR (500 MHz, CDCl₃) δ 8.27 (s, 1H), 7.80 (t, *J* = 8.0 Hz, 1H), 7.70 (d, *J* = 8.4 Hz, 2H), 7.67 (d, *J* = 7.9 Hz, 1H), 7.57 (d, *J* = 8.7 Hz, 1H), 7.25 (m, 1H), 6.97 (d, *J* = 2.4 Hz, 1H), 6.92 (d, *J* = 8.5 Hz, 2H), 6.81 (dd, *J* = 8.8, 2.4 Hz, 1H), 6.13 (d, *J* = 8.1 Hz, 1H), 5.84–5.77 (m, 1H), 4.15 (d, *J* = 8.1 Hz, 1H), 4.05 (s, 1H), 3.50 (t, *J* = 11.3 Hz, 2H), 3.32 (t, *J* = 5.0 Hz, 4H), 2.99–2.78 (m, 5H), 2.61 (m, 4H), 2.34 (m, 3H), 1.91 (d, *J* = 12.7 Hz, 2H), 1.72 (m, 2H), 1.61 (m, 1H), 1.27 (s, 6H), 1.22 (s, 6H); ¹³C NMR (101 MHz, CDCl₃) δ 170.92, 168.11, 167.14, 162.66, 154.07, 153.57, 152.76, 146.83, 138.27, 135.51, 135.08, 128.27, 120.75, 116.77, 116.38, 114.25, 114.19, 111.26, 105.01, 84.91, 77.25, 64.53, 58.44, 58.17, 53.61, 53.38, 47.86, 40.32, 33.05, 31.09, 30.96, 23.61, 23.53, 23.43; LC/MS (M + H)⁺ (*m/z*) 820.1, (M – H)[–] (*m/z*) 818.0.

4.1.32. Synthesis of *N*-(((1*R*,3*R*)-3-(3-chloro-4-cyanophenoxy)-2,2,4,4-tetramethylcyclobutyl)-4-(4-(7-(3-(2,6-dioxopiperidin-3-yl)-4-oxo-3,4-dihydrobenzo[d][1,2,3]triazin-5-yl)-7-azaspiro[3.5] nonan-2-yl)piperazin-1-yl)benzamide (**29b**)

Similar procedure of **29a** was performed to give **29b** (48 mg, 44%) as a yellow solid. ¹H NMR (500 MHz, CDCl₃) δ 8.51 (s, 1H), 7.79 (t, *J* = 8.0 Hz, 1H), 7.70 (d, *J* = 8.5 Hz, 2H), 7.66 (d, *J* = 7.9 Hz, 1H), 7.56 (d, *J* = 8.7 Hz, 1H), 7.25 (d, *J* = 8.2 Hz, 1H), 6.97 (d, *J* = 2.3 Hz, 1H), 6.92 (d, *J* = 8.6 Hz, 2H), 6.81 (dd, *J* = 9.0, 2.4 Hz, 1H), 6.13 (d, *J* = 8.1 Hz, 1H), 5.81 (dd, *J* = 11.8, 5.3 Hz, 1H), 4.15 (d, *J* = 8.0 Hz, 1H), 4.05 (s, 1H), 3.34 (t, *J* = 5.0 Hz, 4H), 3.08 (d, *J* = 34.9 Hz, 4H), 2.99–2.77 (m, 4H), 2.52 (m, 4H), 2.35 (m, 1H), 2.11 (dd, *J* = 11.3, 7.5 Hz, 2H), 1.89 (t, *J* = 5.3 Hz, 2H), 1.83 (m, 2H), 1.77 (m, 2H), 1.26 (s, 6H), 1.22 (s, 6H); ¹³C NMR (101 MHz, CDCl₃) δ 171.01, 168.22, 167.12, 162.66, 154.04, 152.67, 146.82, 138.26, 135.47, 135.07, 128.28, 120.76, 116.77, 116.36, 114.36, 114.19, 111.22, 105.01, 84.92, 77.26, 58.46, 55.32, 50.47, 50.02, 49.52, 47.50, 40.32, 39.55, 36.74, 31.10, 31.01, 23.61, 23.52; LC/MS (M + H)⁺ (*m/z*) 846.1, (M – H)[–] (*m/z*) 844.0.

4.1.33. Synthesis of *N*-(((1*R*,3*R*)-3-(3-chloro-4-cyanophenoxy)-2,2,4,4-tetramethylcyclobutyl)-4-(4-(2-(1-(3-(2,6-dioxopiperidin-3-yl)-4-oxo-3,4-dihydrobenzo[d][1,2,3]triazin-5-yl)piperidin-4-yl) ethyl)piperazin-1-yl)benzamide (**29c**)

Similar procedure of **29a** was performed to give **29c** (55 mg, 51%) as a pink solid. ¹H NMR (500 MHz, CDCl₃) δ 8.20 (s, 1H), 7.80 (t, *J* = 8.0 Hz, 1H), 7.71 (d, *J* = 8.5 Hz, 2H), 7.67 (d, *J* = 7.9 Hz, 1H), 7.57 (d,

$J = 8.7$ Hz, 1H), 7.25 (d, $J = 8.4$ Hz, 1H), 6.97 (d, $J = 2.4$ Hz, 1H), 6.92 (d, $J = 8.5$ Hz, 2H), 6.81 (m, 1H), 6.13 (d, $J = 8.1$ Hz, 1H), 5.81 (dd, $J = 11.7, 5.4$ Hz, 1H), 4.15 (d, $J = 8.0$ Hz, 1H), 4.05 (s, 1H), 3.48 (m, 5H), 3.01–2.63 (m, 10H), 2.36 (m, 1H), 1.83 (m, 2H), 1.65 (m, 5H), 1.27 (m, 8H), 1.22 (s, 6H); ^{13}C NMR (101 MHz, CDCl_3) δ 171.09, 168.29, 167.05, 162.66, 154.08, 152.69, 146.80, 138.26, 135.53, 135.08, 128.36, 120.88, 120.80, 116.78, 116.37, 114.70, 114.19, 111.27, 105.01, 84.89, 77.27, 58.50, 58.05, 56.00, 53.55, 53.37, 52.54, 47.16, 40.33, 33.84, 32.24, 31.11, 23.62, 23.53, 23.45; LC/MS ($\text{M} + \text{H}$) $^+$ (m/z) 834.14, ($\text{M} - \text{H}$) $^-$ (m/z) 832.31.

4.1.34. Synthesis of *N*-((1*R*,3*R*)-3-(3-chloro-4-cyanophenoxy)-2,2,4,4-tetramethylcyclobutyl)-4-(4-((1-(3-(2,6-dioxopiperidin-3-yl)-4-oxo-3,4-dihydrobenzo[d][1,2,3]triazin-6-yl)piperidin-4-yl)methyl)piperazin-1-yl)benzamide (30a)

Similar procedure of **29a** was performed to give **30a** (45 mg, 41%) as a yellow solid. ^1H NMR (500 MHz, CDCl_3) δ 8.36 (s, 1H), 7.98 (d, $J = 9.1$ Hz, 1H), 7.70 (d, $J = 8.4$ Hz, 2H), 7.57 (d, $J = 8.7$ Hz, 1H), 7.52 (d, $J = 2.8$ Hz, 1H), 7.45 (dd, $J = 9.2, 2.9$ Hz, 1H), 6.99–6.94 (m, 1H), 6.92 (d, $J = 8.5$ Hz, 2H), 6.81 (dd, $J = 8.2, 2.3$ Hz, 1H), 6.14 (d, $J = 8.1$ Hz, 1H), 5.77 (dd, $J = 11.6, 5.4$ Hz, 1H), 4.15 (d, $J = 8.1$ Hz, 1H), 4.07 (s, 1H), 4.05 (m, 2H), 3.32 (t, $J = 5.0$ Hz, 4H), 3.02 (t, $J = 12.5$ Hz, 2H), 2.98–2.81 (m, 3H), 2.59 (t, $J = 5.0$ Hz, 4H), 2.40–2.34 (m, 1H), 2.28 (d, $J = 7.1$ Hz, 2H), 1.99–1.92 (m, 2H), 1.86 (m, 1H), 1.33 (m, 2H), 1.27 (s, 6H), 1.22 (s, 6H); ^{13}C NMR (101 MHz, CDCl_3) δ 171.03, 168.09, 167.13, 162.66, 156.09, 153.51, 153.29, 138.27, 136.37, 135.08, 130.34, 128.28, 123.93, 121.73, 121.51, 116.77, 116.37, 114.28, 114.19, 105.33, 105.01, 84.90, 64.23, 58.46, 58.12, 53.37, 47.79, 40.32, 33.30, 31.05, 30.13, 23.61, 23.52, 23.27; LC/MS ($\text{M} + \text{H}$) $^+$ (m/z) 820.1, ($\text{M} - \text{H}$) $^-$ (m/z) 818.1.

4.1.35. Synthesis of *N*-((1*R*,3*R*)-3-(3-chloro-4-cyanophenoxy)-2,2,4,4-tetramethylcyclobutyl)-4-(4-(7-(3-(2,6-dioxopiperidin-3-yl)-4-oxo-3,4-dihydrobenzo[d][1,2,3]triazin-6-yl)-7-azaspiro[3.5]nonan-2-yl)piperazin-1-yl)benzamide (30b)

Similar procedure of **29a** was performed to give **30b** (45 mg, 41%) as a yellow solid. ^1H NMR (500 MHz, CDCl_3) δ 8.63 (s, 1H), 7.98 (d, $J = 9.1$ Hz, 1H), 7.70 (d, $J = 8.4$ Hz, 2H), 7.56 (d, $J = 8.7$ Hz, 1H), 7.51 (d, $J = 2.8$ Hz, 1H), 7.43 (dd, $J = 9.2, 2.8$ Hz, 1H), 6.97 (m, 1H), 6.92 (d, $J = 8.5$ Hz, 2H), 6.81 (dd, $J = 8.8, 2.4$ Hz, 1H), 6.14 (d, $J = 8.1$ Hz, 1H), 5.76 (dd, $J = 11.7, 5.4$ Hz, 1H), 4.15 (d, $J = 8.1$ Hz, 1H), 4.05 (s, 1H), 3.53–3.46 (m, 4H), 3.34 (t, $J = 4.9$ Hz, 4H), 2.98–2.79 (m, 4H), 2.52 (m, 4H), 2.37 (m, 1H), 2.11 (dd, $J = 11.4, 7.5$ Hz, 2H), 1.76 (m, 4H), 1.72 (t, $J = 5.6$ Hz, 2H), 1.26 (s, 6H), 1.22 (s, 6H); ^{13}C NMR (101 MHz, CDCl_3) δ 171.13, 168.19, 167.11, 162.66, 156.06, 153.19, 138.26, 136.34, 135.08, 130.34, 128.29, 121.63, 121.52, 116.77, 116.36, 114.38, 114.19, 105.27, 105.01, 84.91, 77.26, 58.47, 58.16, 55.08, 49.49, 47.49, 44.93, 44.77, 40.32, 38.62, 36.46, 35.96, 31.49, 31.07, 23.61, 23.52, 23.26; LC/MS ($\text{M} + \text{H}$) $^+$ (m/z) 846.1, ($\text{M} - \text{H}$) $^-$ (m/z) 844.0.

4.1.36. Synthesis of *N*-((1*R*,3*R*)-3-(3-chloro-4-cyanophenoxy)-2,2,4,4-tetramethylcyclobutyl)-4-(4-(2-(1-(3-(2,6-dioxopiperidin-3-yl)-4-oxo-3,4-dihydrobenzo[d][1,2,3]triazin-6-yl)piperidin-4-yl)ethyl)piperazin-1-yl)benzamide (30c)

Similar procedure of **29a** was performed to give **30c** (48 mg, 44%) as a white solid. ^1H NMR (500 MHz, CDCl_3) δ 8.10 (s, 1H), 7.98 (d, $J = 9.1$ Hz, 1H), 7.70 (d, $J = 8.4$ Hz, 2H), 7.57 (d, $J = 8.7$ Hz, 1H), 7.51 (d, $J = 2.8$ Hz, 1H), 7.43 (dd, $J = 9.1, 2.9$ Hz, 1H), 6.96 (m, 1H), 6.92 (d, $J = 8.5$ Hz, 2H), 6.81 (dd, $J = 8.6, 2.1$ Hz, 1H), 6.11 (d, $J = 8.1$ Hz, 1H), 5.76 (dd, $J = 11.5, 5.4$ Hz, 1H), 4.15 (d, $J = 8.1$ Hz, 1H), 4.09–3.98 (m, 3H), 3.32 (t, $J = 4.8$ Hz, 4H), 2.98 (m, 4H), 2.84 (m, 1H), 2.61 (m, 4H), 2.47 (t, $J = 7.6$ Hz, 2H), 2.38 (m, 1H), 1.87 (d, $J = 13.1$ Hz, 2H), 1.66 (m, 1H), 1.53 (m, 2H), 1.40–1.33 (m, 2H), 1.26 (s, 6H), 1.22 (s, 6H); ^{13}C NMR (101 MHz, CDCl_3) δ 171.09, 168.15, 167.11, 162.66, 156.09, 153.45, 153.22, 138.26, 136.33, 135.07, 130.34, 128.28, 124.00, 121.64,

116.77, 116.36, 114.31, 105.24, 105.02, 84.92, 77.26, 58.46, 58.12, 55.92, 52.97, 47.90, 40.32, 34.22, 33.25, 31.66, 31.07, 23.61, 23.52, 23.27; LC/MS ($\text{M} + \text{H}$) $^+$ (m/z) 834.20, ($\text{M} - \text{H}$) $^-$ (m/z) 832.31.

4.1.37. Synthesis of *N*-((1*R*,3*R*)-3-(3-chloro-4-cyanophenoxy)-2,2,4,4-tetramethylcyclobutyl)-4-(4-(2-(1-(3-(2,6-dioxopiperidin-3-yl)-4-oxo-3,4-dihydrobenzo[d][1,2,3]triazin-6-yl)piperidin-4-yl)oxy)ethyl)piperazin-1-yl)benzamide (30d)

Similar procedure of **29a** was performed to give **30d** (42 mg, 62%) as an ivory solid. ^1H NMR (500 MHz, CDCl_3) δ 8.33 (s, 1H), 7.99 (d, $J = 9.2$ Hz, 1H), 7.69 (d, $J = 8.4$ Hz, 2H), 7.56 (d, $J = 8.7$ Hz, 1H), 7.55–7.51 (m, 1H), 7.44 (dd, $J = 9.2, 2.8$ Hz, 1H), 6.99–6.95 (m, 1H), 6.91 (d, $J = 8.5$ Hz, 2H), 6.84–6.77 (m, 1H), 6.12 (d, $J = 8.1$ Hz, 1H), 5.81–5.73 (m, 1H), 4.15 (d, $J = 8.1$ Hz, 1H), 4.04 (s, 1H), 3.83–3.74 (m, 2H), 3.70 (t, $J = 5.8$ Hz, 2H), 3.66–3.59 (m, 1H), 3.38–3.34 (m, 1H), 3.34–3.26 (m, 5H), 3.00–2.78 (m, 3H), 2.75–2.64 (m, 6H), 2.42–2.33 (m, 1H), 2.04–1.94 (m, 2H), 1.80–1.71 (m, 2H), 1.26 (s, 6H), 1.22 (s, 6H); ^{13}C NMR (126 MHz, CDCl_3) δ 171.20, 168.23, 167.10, 162.61, 156.02, 153.40, 152.95, 138.21, 136.39, 135.06, 130.34, 128.25, 123.89, 121.67, 121.44, 116.72, 116.40, 114.25, 114.14, 105.31, 104.90, 84.78, 74.14, 66.05, 58.37, 57.99, 53.31, 47.69, 44.94, 40.26, 31.07, 30.27, 23.58, 23.49, 23.23; LC/MS ($\text{M} + \text{H}$) $^+$ (m/z) 850.14, ($\text{M} - \text{H}$) $^-$ (m/z) 848.45.

4.1.38. Synthesis of *N*-((1*r*,3*r*)-3-(3-chloro-4-cyanophenoxy)-2,2,4,4-tetramethylcyclobutyl)-4-(4-(1-(3-(2,6-dioxopiperidin-3-yl)-4-oxo-3,4-dihydrobenzo[d][1,2,3]triazin-7-yl)piperidin-4-yl)methyl)piperazin-1-yl)benzamide (31a)

Similar procedure of **29a** was performed to give **31a** (4 mg, 20%) as a yellow solid. ^1H NMR (500 MHz, CDCl_3) δ 8.13 (d, $J = 9.1$ Hz, 2H), 7.73–7.67 (m, 2H), 7.57 (d, $J = 8.7$ Hz, 1H), 7.38 (d, $J = 2.6$ Hz, 1H), 7.32 (dd, $J = 9.1, 2.6$ Hz, 1H), 6.97 (d, $J = 2.4$ Hz, 1H), 6.95–6.90 (m, 2H), 6.81 (dd, $J = 8.7, 2.4$ Hz, 1H), 6.13 (d, $J = 8.1$ Hz, 1H), 5.79 (dd, $J = 11.7, 5.3$ Hz, 1H), 4.15 (d, $J = 8.1$ Hz, 1H), 4.04 (m, 3H), 3.32 (m, 4H), 3.09–2.84 (m, 5H), 2.60 (m, 4H), 2.42–2.35 (m, 1H), 2.30 (d, $J = 7.1$ Hz, 2H), 1.96 (d, $J = 13.3$ Hz, 2H), 1.34 (m, 2H), 1.27 (s, 6H), 1.25 (m, 1H), 1.22 (s, 6H); LC/MS ($\text{M} + \text{H}$) $^+$ (m/z) 820.2, ($\text{M} - \text{H}$) $^-$ (m/z) 818.1.

4.1.39. Synthesis of *N*-((1*R*,3*R*)-3-(3-chloro-4-cyanophenoxy)-2,2,4,4-tetramethylcyclobutyl)-4-(4-(1-(3-(2,6-dioxopiperidin-3-yl)-4-oxo-3,4-dihydrobenzo[d][1,2,3]triazin-6-yl)glycyl)piperidin-4-yl)methyl)piperazin-1-yl)benzamide (32a)

To a solution of **28a** (50 mg, 0.0832 mmol), **20a** (33 mg, 0.0998 mmol), EDCl·HCl (18 mg, 0.0915 mmol), and HOBT (12 mg, 0.0915 mmol) in DMF (5 mL) was added DIPEA (0.072 mL, 0.416 mmol). The reaction mixture was stirred at room temperature for 12 h. The reaction mixture was diluted with water and extracted with ethyl acetate. The organic layer was washed with brine, dried over Na_2SO_4 , and concentrated under reduced pressure. The residue was purified by column chromatography to afford **32a** (50 mg, 68%) as a white solid. ^1H NMR (500 MHz, CDCl_3) δ 9.03 (s, 1H), 7.90 (d, $J = 8.9$ Hz, 1H), 7.70 (d, $J = 8.5$ Hz, 2H), 7.56 (d, $J = 8.7$ Hz, 1H), 7.25 (dd, $J = 9.0, 2.6$ Hz, 1H), 7.13 (d, $J = 2.7$ Hz, 1H), 6.97 (d, $J = 2.4$ Hz, 1H), 6.91 (d, $J = 8.6$ Hz, 2H), 6.81 (dd, $J = 8.7, 2.4$ Hz, 1H), 6.18 (d, $J = 8.2$ Hz, 1H), 6.12 (t, $J = 3.8$ Hz, 1H), 5.81 (m, 1H), 4.63 (d, $J = 13.1$ Hz, 1H), 4.15 (d, $J = 8.1$ Hz, 1H), 4.05 (s, 1H), 4.00 (m, 2H), 3.83 (d, $J = 13.2$ Hz, 1H), 3.31 (t, $J = 4.8$ Hz, 4H), 3.06 (t, $J = 12.8$ Hz, 1H), 2.96–2.81 (m, 3H), 2.71 (t, $J = 12.6$ Hz, 1H), 2.58 (t, $J = 5.1$ Hz, 4H), 2.39–2.33 (m, 1H), 2.26 (d, $J = 7.0$ Hz, 2H), 1.94 (m, 3H), 1.27 (s, 6H), 1.22 (s, 6H), 1.20–1.10 (m, 2H); ^{13}C NMR (101 MHz, CDCl_3) δ 171.53, 168.52, 167.18, 165.71, 162.66, 156.13, 153.47, 150.51, 138.23, 136.87, 135.09, 130.26, 128.30, 123.94, 122.81, 121.91, 116.78, 116.38, 114.26, 114.19, 104.97, 101.30, 84.89, 77.30, 64.04, 58.47, 58.16, 58.06, 53.34, 47.77, 44.51, 44.38, 42.60, 40.33, 33.56, 31.04, 30.30, 23.62,

23.51, 23.29; LC/MS (M + H)⁺ (m/z) 877.1, (M – H)[–] (m/z) 875.0.

4.1.40. Synthesis of N-((1R,3R)-3-(3-chloro-4-cyanophenoxy)-2,2,4,4-tetramethylcyclobutyl)-4-(4-((1-(1-(3-(2,6-dioxopiperidin-3-yl)-4-oxo-3,4-dihydrobenzo[d][1,2,3]triazin-6-yl)azetidine-3-carbonyl)piperidin-4-yl)methyl)piperazin-1-yl)benzamide (32b)

Similar procedure of **32a** was performed to give **32b** (50 mg, 66%) as a white solid. ¹H NMR (400 MHz, CDCl₃) δ 8.10 (s, 1H), 7.97 (d, J = 8.8 Hz, 1H), 7.70 (d, J = 8.6 Hz, 2H), 7.57 (d, J = 8.7 Hz, 1H), 7.05 (d, J = 2.6 Hz, 1H), 6.99–6.86 (m, 4H), 6.81 (dd, J = 8.7, 2.4 Hz, 1H), 6.11 (d, J = 8.1 Hz, 1H), 5.80–5.71 (m, 1H), 4.63 (d, J = 13.5 Hz, 1H), 4.38–4.24 (m, 4H), 4.15 (d, J = 8.0 Hz, 1H), 4.04 (s, 1H), 3.79 (p, J = 7.5 Hz, 1H), 3.59 (d, J = 13.6 Hz, 1H), 3.31 (t, J = 5.0 Hz, 4H), 3.12–3.02 (m, 1H), 3.00–2.80 (m, 3H), 2.71–2.53 (m, 5H), 2.37 (m, 1H), 2.27 (d, J = 7.0 Hz, 2H), 1.93 (m, 1H), 1.86 (m, 2H), 1.26 (s, 6H), 1.22 (s, 6H), 1.13 (m, 2H); ¹³C NMR (126 MHz, CDCl₃) δ 171.12, 168.88, 168.12, 167.08, 162.59, 155.85, 153.44, 152.80, 138.21, 136.42, 135.05, 130.42, 128.24, 123.85, 121.35, 118.29, 116.71, 116.39, 114.18, 104.90, 101.98, 84.77, 64.06, 58.37, 57.89, 53.72, 53.30, 47.77, 45.48, 42.31, 40.27, 33.59, 32.14, 31.39, 31.02, 30.32, 23.59, 23.50, 23.26; LC/MS (M + H)⁺ (m/z) 903.1, (M – H)[–] (m/z) 901.0.

4.1.41. Synthesis of N-((1R,3R)-3-(3-chloro-4-cyanophenoxy)-2,2,4,4-tetramethylcyclobutyl)-4-(4-((1-(1-(3-(2,6-dioxopiperidin-3-yl)-4-oxo-3,4-dihydrobenzo[d][1,2,3]triazin-6-yl)piperidine-4-carbonyl)piperidin-4-yl)methyl)piperazin-1-yl)benzamide (32c)

Similar procedure of **32a** was performed to give **32c** (48 mg, 62%) as a pink solid. ¹H NMR (400 MHz, CDCl₃) δ 8.05–7.95 (m, 2H), 7.69 (d, J = 8.8 Hz, 2H), 7.57 (d, J = 8.7 Hz, 1H), 7.52 (d, J = 2.9 Hz, 1H), 7.45 (dd, J = 9.2, 2.9 Hz, 1H), 6.96 (d, J = 2.4 Hz, 1H), 6.94–6.88 (m, 2H), 6.81 (dd, J = 8.8, 2.4 Hz, 1H), 6.11 (d, J = 8.1 Hz, 1H), 5.77 (dd, J = 11.5, 5.3 Hz, 1H), 4.64 (d, J = 13.2 Hz, 1H), 4.15 (d, J = 8.1 Hz, 1H), 4.10–4.03 (m, 3H), 3.95 (m, 1H), 3.30 (t, J = 5.1 Hz, 4H), 3.10 (t, J = 12.4 Hz, 3H), 2.96 (m, 2H), 2.88–2.75 (m, 2H), 2.58 (m, 5H), 2.41–2.34 (m, 1H), 2.27 (d, J = 6.9 Hz, 2H), 1.88 (m, 7H), 1.26 (s, 6H), 1.22 (s, 6H), 1.13 (m, 2H); ¹³C NMR (101 MHz, CDCl₃) δ 172.35, 171.34, 168.30, 167.18, 162.67, 156.02, 153.47, 153.16, 138.21, 136.52, 135.08, 130.27, 128.30, 123.92, 121.81, 121.42, 116.78, 116.38, 114.25, 114.19, 105.44, 104.94, 84.89, 77.31, 64.16, 58.47, 58.02, 53.33, 47.79, 47.09, 45.64, 42.11, 40.33, 37.85, 31.76, 31.06, 30.51, 28.06, 27.80, 23.62, 23.50, 23.29; LC/MS (M + H)⁺ (m/z) 931.1, (M – H)[–] (m/z) 929.1.

4.1.42. Synthesis of N-((1R,3R)-3-(3-chloro-4-cyanophenoxy)-2,2,4,4-tetramethylcyclobutyl)-4-(4-((1-(2-((3-(2,6-dioxopiperidin-3-yl)-4-oxo-3,4-dihydrobenzo[d][1,2,3]triazin-6-yl)oxy)acetyl)piperidin-4-yl)methyl)piperazin-1-yl)benzamide (32d)

Similar procedure of **32a** was performed to give **32d** (15 mg, 26%) as a yellow solid. ¹H NMR (500 MHz, CDCl₃) δ 8.15 (d, J = 8.1 Hz, 2H), 7.69 (d, J = 8.4 Hz, 2H), 7.64 (d, J = 7.3 Hz, 2H), 7.56 (d, J = 8.7 Hz, 1H), 6.96 (m, 1H), 6.91 (d, J = 8.5 Hz, 2H), 6.81 (d, J = 8.8 Hz, 1H), 6.11 (d, J = 8.1 Hz, 1H), 5.84–5.72 (m, 1H), 4.90 (m, 2H), 4.58 (d, J = 13.2 Hz, 1H), 4.15 (d, J = 8.1 Hz, 1H), 4.04 (s, 1H), 3.91–3.78 (m, 1H), 3.48 (q, J = 6.9 Hz, 1H), 3.31 (m, 4H), 3.13 (t, J = 12.9 Hz, 1H), 3.04–2.90 (m, 2H), 2.89–2.82 (m, 1H), 2.68 (t, J = 13.0 Hz, 1H), 2.58 (m, 4H), 2.39 (m, 1H), 2.27 (m, 2H), 1.95 (d, J = 13.2 Hz, 1H), 1.86 (m, 1H), 1.26 (s, 6H), 1.22 (s, 6H), 1.20 (m, 2H); LC/MS (M + H)⁺ (m/z) 878.2, (M – H)[–] (m/z) 876.1.

4.1.43. Synthesis of N-((1R,3R)-3-(3-chloro-4-cyanophenoxy)-2,2,4,4-tetramethylcyclobutyl)-4-(4-(7-((3-(2,6-dioxopiperidin-3-yl)-4-oxo-3,4-dihydrobenzo[d][1,2,3]triazin-6-yl)glycyl)-7-azaspiro[3.5]nonan-2-yl)piperazin-1-yl)benzamide (33a)

Similar procedure of **32a** was performed to give **33a** (42 mg, 55%) as a white solid. ¹H NMR (500 MHz, DMSO-d₆) δ 11.15 (s, 1H),

7.92 (d, J = 8.8 Hz, 2H), 7.76 (d, J = 8.6 Hz, 2H), 7.55–7.48 (m, 2H), 7.25 (t, J = 5.2 Hz, 1H), 7.22 (d, J = 2.4 Hz, 1H), 7.14 (m, 1H), 7.01 (dd, J = 8.8, 2.4 Hz, 1H), 6.98 (d, J = 8.6 Hz, 2H), 5.87 (m, 1H), 4.33 (s, 1H), 4.18–4.14 (m, 2H), 4.06 (d, J = 9.1 Hz, 1H), 3.48 (m, 2H), 3.40 (m, 2H), 3.26 (m, 4H), 3.02–2.92 (m, 1H), 2.80–2.63 (m, 3H), 2.40 (m, 4H), 2.22 (m, 1H), 2.03 (m, 2H), 1.64 (m, 3H), 1.55 (m, 2H), 1.45 (m, 1H), 1.23 (s, 6H), 1.13 (s, 6H); ¹³C NMR (101 MHz, DMSO-d₆) δ 173.22, 170.32, 167.24, 166.71, 163.11, 155.54, 153.42, 152.51, 137.33, 136.55, 136.03, 129.97, 129.34, 124.25, 121.81, 117.29, 116.76, 115.14, 114.01, 104.07, 79.65, 58.51, 55.38, 54.88, 54.78, 49.45, 47.54, 44.59, 41.80, 41.66, 36.52, 31.70, 31.24, 24.44, 23.60, 23.19; LC/MS (M + H)⁺ (m/z) 903.1, (M – H)[–] (m/z) 901.0.

4.1.44. Synthesis of N-((1Rr,3R)-3-(3-chloro-4-cyanophenoxy)-2,2,4,4-tetramethylcyclobutyl)-4-(4-(7-(1-(3-(2,6-dioxopiperidin-3-yl)-4-oxo-3,4-dihydrobenzo[d][1,2,3]triazin-6-yl)azetidine-3-carbonyl)-7-azaspiro[3.5]nonan-2-yl)piperazin-1-yl)benzamide (33b)

Similar procedure of **32a** was performed to give **33b** (45 mg, 61%) as a white solid. ¹H NMR (500 MHz, DMSO-d₆) δ 11.20 (s, 1H), 8.07 (dd, J = 8.9, 1.4 Hz, 1H), 7.97 (d, J = 8.7 Hz, 1H), 7.81 (d, J = 8.5 Hz, 2H), 7.58 (d, J = 9.2 Hz, 1H), 7.27 (d, J = 2.4 Hz, 1H), 7.21 (dt, J = 8.9, 2.4 Hz, 1H), 7.07 (dd, J = 8.8, 2.4 Hz, 1H), 7.04 (d, J = 8.7 Hz, 2H), 6.96 (t, J = 2.3 Hz, 1H), 5.95 (dd, J = 12.1, 5.6 Hz, 1H), 4.38 (s, 1H), 4.35 (q, J = 8.1 Hz, 2H), 4.24 (m, 2H), 4.12 (d, J = 9.1 Hz, 1H), 3.98 (m, 1H), 3.54 (m, 1H), 3.48 (m, 1H), 3.29 (m, 6H), 3.06–2.96 (m, 1H), 2.83–2.78 (m, 1H), 2.76–2.68 (m, 2H), 2.45 (m, 4H), 2.29 (m, 1H), 2.06 (m, 2H), 1.67 (m, 3H), 1.58 (m, 2H), 1.50 (m, 1H), 1.28 (s, 6H), 1.19 (s, 6H); ¹³C NMR (101 MHz, DMSO-d₆) δ 173.20, 170.30, 169.35, 167.23, 163.11, 155.32, 153.41, 153.32, 137.33, 136.54, 136.02, 130.43, 129.34, 124.25, 121.46, 119.21, 117.29, 116.75, 115.13, 114.01, 104.07, 101.20, 84.40, 79.65, 58.51, 54.85, 49.45, 47.54, 40.78, 36.51, 31.78, 31.74, 31.24, 24.44, 23.60, 23.22; LC/MS (M + H)⁺ (m/z) 929.0, (M – H)[–] (m/z) 927.0.

4.1.45. Synthesis of N-((1R,3R)-3-(3-chloro-4-cyanophenoxy)-2,2,4,4-tetramethylcyclobutyl)-4-(4-(7-(1-(3-(2,6-dioxopiperidin-3-yl)-4-oxo-3,4-dihydrobenzo[d][1,2,3]triazin-6-yl)piperidine-4-carbonyl)-7-azaspiro[3.5]nonan-2-yl)piperazin-1-yl)benzamide (33c)

Similar procedure of **32a** was performed to give **33c** (170 mg, 56%) as a white solid. ¹H NMR (400 MHz, CDCl₃) δ 8.20 (s, 1H), 7.99 (d, J = 9.1 Hz, 1H), 7.70 (d, J = 8.7 Hz, 2H), 7.56 (d, J = 8.7 Hz, 1H), 7.52 (d, J = 2.8 Hz, 1H), 7.45 (dd, J = 9.3, 2.8 Hz, 1H), 6.96 (d, J = 2.4 Hz, 1H), 6.94–6.87 (m, 2H), 6.81 (dd, J = 8.8, 2.4 Hz, 1H), 6.11 (d, J = 8.1 Hz, 1H), 5.77 (dd, J = 11.5, 5.4 Hz, 1H), 4.15 (d, J = 8.1 Hz, 1H), 4.06 (m, 3H), 3.64–3.39 (m, 4H), 3.32 (t, J = 5.0 Hz, 4H), 3.09 (t, J = 12.7 Hz, 2H), 3.00–2.72 (m, 5H), 2.49 (t, J = 4.9 Hz, 4H), 2.42–2.32 (m, 1H), 2.09 (m, 2H), 1.94 (m, 2H), 1.85 (m, 2H), 1.74 (m, 2H), 1.64 (m, 2H), 1.56 (m, 2H), 1.26 (s, 6H), 1.22 (s, 6H); ¹³C NMR (101 MHz, DMSO-d₆) δ 173.21, 172.41, 170.29, 167.23, 163.11, 155.45, 153.42, 153.21, 137.33, 136.55, 136.02, 130.34, 129.33, 124.24, 122.55, 121.53, 117.29, 116.76, 115.14, 114.01, 104.33, 104.07, 84.40, 79.65, 58.51, 49.46, 47.54, 46.94, 40.78, 37.25, 36.60, 31.82, 31.23, 28.01, 24.44, 23.60, 23.20; LC/MS (M + H)⁺ (m/z) 957.1, (M – H)[–] (m/z) 955.0.

4.1.46. Synthesis of N-((1R,3R)-3-(3-chloro-4-cyanophenoxy)-2,2,4,4-tetramethylcyclobutyl)-4-(4-(7-(2-((3-(2,6-dioxopiperidin-3-yl)-4-oxo-3,4-dihydrobenzo[d][1,2,3]triazin-6-yl)oxy)acetyl)-7-azaspiro[3.5]nonan-2-yl)piperazin-1-yl)benzamide (33d)

Similar procedure of **32a** was performed to give **33d** (13 mg, 22%) as a white solid. ¹H NMR (300 MHz, CDCl₃) δ 8.34 (s, 1H), 8.14 (d, J = 9.8 Hz, 1H), 7.66 (m, 4H), 7.57 (d, J = 8.7 Hz, 1H), 6.96 (d, J = 2.4 Hz, 1H), 6.92 (d, J = 8.5 Hz, 2H), 6.81 (dd, J = 8.7, 2.4 Hz, 1H),

6.12 (d, $J = 8.1$ Hz, 1H), 5.79 (m, 1H), 4.89 (d, $J = 2.7$ Hz, 2H), 4.15 (d, $J = 8.1$ Hz, 1H), 4.04 (s, 1H), 3.56 (m, 1H), 3.44 (m, 1H), 3.33 (m, 5H), 3.14 (m, 1H), 3.01–2.88 (m, 2H), 2.83–2.72 (m, 1H), 2.49 (m, 4H), 2.43–2.34 (m, 1H), 2.16–1.98 (m, 4H), 1.74 (m, 5H), 1.26 (s, 6H), 1.22 (s, 6H); LC/MS (M + H)⁺ (m/z) 904.1, (M – H)[–] (m/z) 902.0.

4.1.47. *Synthesis of N-((1R,3R)-3-(3-chloro-4-cyanophenoxy)-2,2,4,4-tetramethylcyclobutyl)-4-(4-(2-(1-((3-(2,6-dioxopiperidin-3-yl)-4-oxo-3,4-dihydrobenzo[d][1,2,3]triazin-6-yl)glycyl)piperidin-4-yl)ethyl)piperazin-1-yl)benzamide (34a)*

Similar procedure of **32a** was performed to give **34a** (45 mg, 62%) as a pink solid. ¹H NMR (500 MHz, CDCl₃) δ 8.31 (m, 1H), 7.95 (d, $J = 8.9$ Hz, 1H), 7.70 (d, $J = 8.4$ Hz, 2H), 7.57 (d, $J = 8.7$ Hz, 1H), 7.26–7.23 (m, 1H), 7.13 (m, 1H), 6.97 (d, $J = 2.4$ Hz, 1H), 6.92 (d, $J = 8.5$ Hz, 2H), 6.81 (dd, $J = 8.8, 2.4$ Hz, 1H), 6.12 (d, $J = 8.1$ Hz, 1H), 6.03 (m, 1H), 5.77 (m, 1H), 4.64 (d, $J = 13.2$ Hz, 1H), 4.15 (d, $J = 8.1$ Hz, 1H), 4.05 (s, 1H), 3.99 (m, 2H), 3.79 (d, $J = 13.7$ Hz, 1H), 3.36 (m, 4H), 3.10 (t, $J = 12.9$ Hz, 1H), 3.01–2.80 (m, 4H), 2.70 (m, 4H), 2.39 (m, 3H), 1.85 (dd, $J = 30.7, 13.2$ Hz, 2H), 1.64 (m, 3H), 1.26 (m, 7H), 1.22 (m, 7H); ¹³C NMR (101 MHz, CDCl₃) δ 171.48, 168.56, 167.10, 165.65, 162.65, 156.11, 150.56, 138.25, 136.87, 135.08, 130.29, 128.35, 122.81, 121.89, 116.77, 116.36, 114.57, 114.19, 105.00, 101.32, 84.88, 77.26, 58.50, 55.66, 52.64, 47.29, 44.47, 42.64, 40.33, 34.21, 32.40, 31.73, 31.10, 23.62, 23.52, 23.32; LC/MS (M + H)⁺ (m/z) 891.1, (M – H)[–] (m/z) 889.0.

4.1.48. *Synthesis of N-((1Rr,3R)-3-(3-chloro-4-cyanophenoxy)-2,2,4,4-tetramethylcyclobutyl)-4-(4-(2-(1-(1-(3-(2,6-dioxopiperidin-3-yl)-4-oxo-3,4-dihydrobenzo[d][1,2,3]triazin-6-yl)azetidone-3-carbonyl)piperidin-4-yl)ethyl)piperazin-1-yl)benzamide (34b)*

Similar procedure of **32a** was performed to give **34b** (35 mg, 47%) as a white solid. ¹H NMR (500 MHz, CDCl₃) δ 8.17 (m, 1H), 7.97 (d, $J = 8.9$ Hz, 1H), 7.70 (d, $J = 8.5$ Hz, 2H), 7.57 (d, $J = 8.8$ Hz, 1H), 7.04 (dd, $J = 5.4, 2.6$ Hz, 1H), 7.00–6.88 (m, 4H), 6.81 (dd, $J = 8.8, 2.4$ Hz, 1H), 6.11 (d, $J = 8.1$ Hz, 1H), 5.82–5.70 (m, 1H), 4.61 (d, $J = 13.2$ Hz, 1H), 4.29 (m, 4H), 4.15 (d, $J = 8.1$ Hz, 1H), 4.04 (s, 1H), 3.78 (m, 1H), 3.57 (d, $J = 13.3$ Hz, 1H), 3.33 (m, 4H), 3.07 (t, $J = 12.8$ Hz, 1H), 2.99–2.89 (m, 2H), 2.89–2.76 (m, 1H), 2.66 (d, $J = 12.4$ Hz, 1H), 2.61 (m, 4H), 2.44 (m, 2H), 2.41–2.34 (m, 1H), 1.82 (dd, $J = 22.0, 13.5$ Hz, 2H), 1.60 (m, 1H), 1.52 (m, 2H), 1.26 (s, 6H), 1.22 (s, 6H), 1.17 (m, 2H); ¹³C NMR (101 MHz, CDCl₃) δ 171.14, 168.86, 168.16, 167.11, 162.66, 155.88, 153.44, 152.86, 138.26, 136.48, 135.07, 130.46, 128.28, 124.03, 121.41, 118.30, 116.77, 116.36, 114.31, 114.19, 105.02, 102.01, 84.92, 58.47, 57.91, 55.83, 53.77, 52.96, 47.78, 45.61, 42.47, 40.32, 34.47, 33.18, 32.95, 32.15, 31.88, 31.05, 23.61, 23.51, 23.31; LC/MS (M + H)⁺ (m/z) 917.24, (M – H)[–] (m/z) 915.48.

4.1.49. *Synthesis of N-((1Rr,3R)-3-(3-chloro-4-cyanophenoxy)-2,2,4,4-tetramethylcyclobutyl)-4-(4-(2-(1-(1-(3-(2,6-dioxopiperidin-3-yl)-4-oxo-3,4-dihydrobenzo[d][1,2,3]triazin-6-yl)piperidine-4-carbonyl)piperidin-4-yl)ethyl)piperazin-1-yl)benzamide (34c)*

Similar procedure of **32a** was performed to give **34c** (35 mg, 47%) as a white solid. ¹H NMR (500 MHz, CDCl₃) δ 8.05 (s, 1H), 8.00 (d, $J = 9.1$ Hz, 1H), 7.70 (d, $J = 8.5$ Hz, 2H), 7.57 (d, $J = 8.7$ Hz, 1H), 7.52 (d, $J = 2.8$ Hz, 1H), 7.45 (dd, $J = 9.2, 2.9$ Hz, 1H), 6.98–6.95 (m, 1H), 6.92 (d, $J = 8.5$ Hz, 2H), 6.81 (dd, $J = 8.7, 2.4$ Hz, 1H), 6.11 (d, $J = 8.1$ Hz, 1H), 5.77 (dd, $J = 11.4, 5.4$ Hz, 1H), 4.62 (d, $J = 13.3$ Hz, 1H), 4.15 (d, $J = 8.1$ Hz, 1H), 4.06 (m, 3H), 3.93 (d, $J = 13.4$ Hz, 1H), 3.32 (m, 4H), 3.09 (m, 3H), 3.01–2.89 (m, 2H), 2.88–2.76 (m, 2H), 2.60 (m, 5H), 2.45 (t, $J = 7.4$ Hz, 2H), 2.39 (m, 1H), 1.96 (m, 2H), 1.86 (m, 3H), 1.78 (d, $J = 13.2$ Hz, 1H), 1.62 (m, 1H), 1.52 (m, 2H), 1.26 (s, 6H), 1.22 (s, 6H), 1.20–1.08 (m, 2H); ¹³C NMR (101 MHz, CDCl₃) δ 172.25, 171.26, 168.25, 167.13, 162.66, 156.02, 153.44, 153.17, 138.23, 136.55,

135.08, 130.29, 128.29, 121.81, 121.43, 116.78, 116.37, 114.29, 114.19, 105.46, 104.98, 84.90, 77.28, 58.46, 58.00, 55.90, 52.95, 47.76, 47.11, 45.76, 42.23, 40.32, 37.81, 34.60, 33.32, 33.22, 32.01, 31.08, 28.04, 27.82, 23.61, 23.51, 23.30; LC/MS (M + H)⁺ (m/z) 945.1, (M – H)[–] (m/z) 943.0.

4.1.50. *Synthesis of N-((1R,3R)-3-(3-chloro-4-cyanophenoxy)-2,2,4,4-tetramethylcyclobutyl)-4-(4-(2-(1-(2-(1-(3-(2,6-dioxopiperidin-3-yl)-4-oxo-3,4-dihydrobenzo[d][1,2,3]triazin-6-yl)oxy)acetyl)piperidin-4-yl)ethyl)piperazin-1-yl)benzamide (34d)*

Similar procedure of **32a** was performed to give **34d** (18 mg, 42%) as a pink solid. ¹H NMR (500 MHz, CDCl₃) δ 8.14 (d, $J = 8.8$ Hz, 1H), 7.70 (d, $J = 8.4$ Hz, 2H), 7.65–7.60 (m, 2H), 7.56 (d, $J = 8.7$ Hz, 1H), 6.97 (d, $J = 2.4$ Hz, 1H), 6.92 (dd, $J = 8.5, 5.4$ Hz, 2H), 6.81 (dd, $J = 8.7, 2.4$ Hz, 1H), 6.15 (d, $J = 8.4$ Hz, 1H), 5.76 (m, 1H), 5.00–4.84 (m, 2H), 4.56 (d, $J = 13.3$ Hz, 1H), 4.15 (d, $J = 8.1$ Hz, 1H), 4.05 (s, 1H), 3.83 (m, 1H), 3.46 (m, 4H), 3.19–2.86 (m, 5H), 2.84–2.46 (m, 6H), 2.42–2.33 (m, 1H), 1.81 (m, 3H), 1.26 (m, 9H), 1.22 (m, 7H), 1.19–1.11 (m, 1H); LC/MS (M + H)⁺ (m/z) 892.0, (M – H)[–] (m/z) 890.0.

4.1.51. *Synthesis of N-((1R,3R)-3-(3-chloro-4-cyanophenoxy)-2,2,4,4-tetramethylcyclobutyl)-4-(4-(2-(1-(1-(3-(2,6-dioxopiperidin-3-yl)-4-oxo-3,4-dihydrobenzo[d][1,2,3]triazin-6-yl)glycyl)piperidin-4-yl)oxy)ethyl)piperazin-1-yl)benzamide (35a)*

Similar procedure of **32a** was performed to give **35a** (26 mg, 48%) as an ivory solid. ¹H NMR (500 MHz, CDCl₃) δ 8.56 (d, $J = 14.4$ Hz, 1H), 7.94 (d, $J = 8.9$ Hz, 1H), 7.69 (d, $J = 8.7$ Hz, 2H), 7.56 (d, $J = 8.7$ Hz, 1H), 7.25 (dd, $J = 8.9, 2.7$ Hz, 1H), 7.13 (d, $J = 2.6$ Hz, 1H), 6.96 (d, $J = 2.4$ Hz, 1H), 6.91 (d, $J = 8.8$ Hz, 2H), 6.81 (dd, $J = 8.7, 2.4$ Hz, 1H), 6.12 (d, $J = 8.1$ Hz, 1H), 6.03 (t, $J = 3.9$ Hz, 1H), 5.79 (dd, $J = 11.5, 5.3$ Hz, 1H), 4.15 (d, $J = 8.1$ Hz, 1H), 4.04 (s, 1H), 4.00 (d, $J = 3.7$ Hz, 2H), 3.90 (m, 1H), 3.66 (m, 4H), 3.59–3.51 (m, 1H), 3.33 (m, 5H), 3.02–2.79 (m, 3H), 2.70 (m, 6H), 2.38 (m, 1H), 1.97–1.82 (m, 2H), 1.78–1.63 (m, 2H), 1.26 (s, 6H), 1.22 (s, 6H); ¹³C NMR (101 MHz, CDCl₃) δ 171.40, 168.44, 167.13, 165.73, 162.66, 156.13, 153.42, 150.45, 138.25, 136.93, 135.07, 130.30, 128.28, 124.02, 122.85, 121.91, 116.77, 116.36, 114.29, 114.19, 105.00, 101.27, 84.91, 77.27, 73.77, 66.19, 58.47, 57.98, 53.33, 47.75, 44.33, 41.44, 40.32, 39.48, 31.19, 31.12, 30.42, 23.61, 23.52, 23.31; LC/MS (M + H)⁺ (m/z) 907.38, (M – H)[–] (m/z) 905.56.

4.1.52. *Synthesis of N-((1R,3R)-3-(3-chloro-4-cyanophenoxy)-2,2,4,4-tetramethylcyclobutyl)-4-(4-(2-(1-(1-(3-(2,6-dioxopiperidin-3-yl)-4-oxo-3,4-dihydrobenzo[d][1,2,3]triazin-6-yl)azetidone-3-carbonyl)piperidin-4-yl)oxy)ethyl)piperazin-1-yl)benzamide (35b)*

Similar procedure of **32a** was performed to give **35b** (13 mg, 43%) as an ivory solid. ¹H NMR (500 MHz, CDCl₃) δ 8.24 (d, $J = 5.2$ Hz, 1H), 7.97 (d, $J = 8.8$ Hz, 1H), 7.73–7.66 (m, 2H), 7.57 (d, $J = 8.7$ Hz, 1H), 7.06–7.02 (m, 1H), 6.96 (d, $J = 2.4$ Hz, 1H), 6.96–6.93 (m, 1H), 6.93–6.89 (m, 2H), 6.81 (dd, $J = 8.7, 2.4$ Hz, 1H), 6.12 (d, $J = 8.1$ Hz, 1H), 5.80–5.72 (m, 1H), 4.32 (t, $J = 7.1$ Hz, 2H), 4.30–4.24 (m, 2H), 4.15 (d, $J = 8.1$ Hz, 1H), 4.04 (s, 1H), 3.94–3.84 (m, 1H), 3.84–3.74 (m, 1H), 3.73–3.63 (m, 2H), 3.64–3.57 (m, 1H), 3.57–3.49 (m, 1H), 3.50–3.42 (m, 1H), 3.38–3.27 (m, 4H), 3.23–3.14 (m, 1H), 3.00–2.78 (m, 3H), 2.76–2.62 (m, 6H), 2.42–2.33 (m, 1H), 1.92–1.80 (m, 2H), 1.71–1.59 (m, 2H), 1.26 (s, 6H), 1.22 (s, 6H); ¹³C NMR (101 MHz, CDCl₃) δ 171.39, 169.01, 168.39, 167.14, 162.67, 155.85, 153.41, 152.81, 138.22, 136.45, 135.08, 130.40, 128.30, 123.99, 121.38, 118.28, 116.79, 116.38, 114.27, 114.18, 104.95, 102.01, 84.90, 77.30, 73.96, 66.13, 58.47, 57.95, 57.85, 53.74, 53.30, 47.71, 42.44, 40.32, 39.25, 32.06, 31.57, 31.10, 30.42, 23.62, 23.51, 23.32; LC/MS (M + H)⁺ (m/z) 933.37, (M – H)[–] (m/z) 931.48.

4.1.53. Synthesis of *N*-((1*R*,3*R*)-3-(3-chloro-4-cyanophenoxy)-2,2,4,4-tetramethylcyclobutyl)-4-(4-(2-((1-(1-(3-(2,6-dioxopiperidin-3-yl)-4-oxo-3,4-dihydrobenzo[d][1,2,3]triazin-6-yl)piperidine-4-carbonyl)piperidin-4-yl)oxy)ethyl)piperazin-1-yl)benzamide (**35c**)

Similar procedure of **32a** was performed to give **35c** (13 mg, 43%) as an ivory solid. ¹H NMR (500 MHz, CDCl₃) δ 8.36 (s, 1H), 7.99 (d, *J* = 9.1 Hz, 1H), 7.73–7.66 (m, 2H), 7.57 (d, *J* = 8.7 Hz, 1H), 7.52 (d, *J* = 2.8 Hz, 1H), 7.45 (dd, *J* = 9.1, 2.8 Hz, 1H), 6.97 (d, *J* = 2.4 Hz, 1H), 6.94–6.88 (m, 2H), 6.81 (dd, *J* = 8.7, 2.4 Hz, 1H), 6.13 (d, *J* = 8.1 Hz, 1H), 5.81–5.73 (m, 1H), 4.15 (d, *J* = 8.1 Hz, 1H), 4.10–4.02 (m, 3H), 3.98–3.89 (m, 1H), 3.81–3.72 (m, 1H), 3.72–3.63 (m, 2H), 3.63–3.56 (m, 1H), 3.41–3.28 (m, 6H), 3.15–3.05 (m, 2H), 3.00–2.88 (m, 2H), 2.88–2.77 (m, 2H), 2.76–2.64 (m, 6H), 2.42–2.33 (m, 1H), 2.01–1.80 (m, 6H), 1.70–1.55 (m, 2H), 1.26 (s, 6H), 1.22 (s, 6H); ¹³C NMR (101 MHz, CDCl₃) δ 172.35, 171.07, 168.10, 167.10, 162.66, 156.01, 153.44, 153.16, 138.26, 136.58, 135.07, 130.33, 128.28, 124.01, 121.83, 121.45, 116.77, 114.29, 114.19, 105.50, 105.02, 84.91, 77.25, 74.35, 66.16, 58.46, 58.02, 53.36, 47.79, 47.10, 42.70, 40.32, 39.13, 37.76, 32.05, 31.07, 30.62, 27.92, 23.61, 23.52, 23.30; LC/MS (M + H)⁺ (*m/z*) 961.45, (M – H)[–] (*m/z*) 959.56.

4.1.54. Synthesis of *N*-((1*R*,3*R*)-3-(3-chloro-4-cyanophenoxy)-2,2,4,4-tetramethylcyclobutyl)-4-(4-(2-((1-(2-(3-(2,6-dioxopiperidin-3-yl)-4-oxo-3,4-dihydrobenzo[d][1,2,3]triazin-6-yl)oxy)acetyl)piperidin-4-yl)oxy)ethyl)piperazin-1-yl)benzamide (**35d**)

Similar procedure of **32a** was performed to give **35d** (7 mg, 21%) as a white solid. ¹H NMR (500 MHz, CDCl₃) δ 8.28 (m, 1H), 8.14 (d, *J* = 8.6 Hz, 1H), 7.70 (d, *J* = 8.4 Hz, 2H), 7.63 (m, 2H), 7.57 (d, *J* = 8.7 Hz, 1H), 6.97 (d, *J* = 2.3 Hz, 1H), 6.92 (d, *J* = 8.5 Hz, 2H), 6.81 (dd, *J* = 8.7, 2.3 Hz, 1H), 6.13 (d, *J* = 8.1 Hz, 1H), 5.78 (dd, *J* = 11.6, 5.4 Hz, 1H), 4.91 (s, 2H), 4.15 (d, *J* = 8.0 Hz, 1H), 4.05 (s, 1H), 3.93–3.60 (m, 5H), 3.51–3.27 (m, 5H), 3.04–2.68 (m, 8H), 2.38 (m, 1H), 1.90 (m, 2H), 1.68 (m, 4H), 1.26 (s, 6H), 1.22 (s, 6H); LC/MS (M + H)⁺ (*m/z*) 908.33, (M – H)[–] (*m/z*) 906.50.

4.1.55. Synthesis of 3-(6-fluoro-4-oxobenzo[d][1,2,3]triazin-3(4*H*)-yl)-1-methylpiperidine-2,6-dione (**36**)

To a solution of **18b** (400 mg, 1.44 mmol) and K₂CO₃ (398 mg, 2.88 mmol) in DMF (5 mL) was added iodomethane (0.135 mL, 2.17 mmol). The reaction mixture was stirred at room temperature for 12 h. The reaction mixture was diluted with water and extracted with ethyl acetate. The organic layer was washed with brine, dried over Na₂SO₄ and concentrated under reduced pressure. The residue was purified by column chromatography to afford **36** (264 mg, 63%) as a white solid. ¹H NMR (500 MHz, DMSO-*d*₆) δ 8.40 (m, 1H), 8.08–8.00 (m, 2H), 6.07 (dd, *J* = 12.8, 5.3 Hz, 1H), 3.05 (m, 4H), 2.85 (m, 1H), 2.71 (m, 1H), 2.33–2.25 (m, 1H).

4.1.56. Synthesis of *tert*-butyl 1-(3-(1-methyl-2,6-dioxopiperidin-3-yl)-4-oxo-3,4-dihydrobenzo[d][1,2,3]triazin-6-yl)piperidine-4-carboxylate (**37**)

To a solution of **36** (100 mg, 0.344 mmol) and *tert*-butyl piperidine-4-carboxylate hydrochloride (114 mg, 0.516 mmol) in DMSO (5 mL) was added DIPEA (0.18 mL, 1.032 mmol). The reaction mixture was stirred at 90 °C for 12 h. The reaction mixture was cooled to room temperature, diluted with water, and extracted with ethyl acetate. The organic layer was washed with brine, dried over Na₂SO₄, and concentrated under reduced pressure. The residue was purified by column chromatography to afford **37** (130 mg, 82%) as a white solid. ¹H NMR (500 MHz, CDCl₃) δ 7.99 (d, *J* = 9.1 Hz, 1H), 7.53 (d, *J* = 2.9 Hz, 1H), 7.44 (dd, *J* = 9.2, 2.9 Hz, 1H), 5.79 (m, 1H), 3.95 (dt, *J* = 13.9, 4.3 Hz, 2H), 3.25 (s, 3H), 3.12 (m, 2H), 3.07–3.01 (m, 1H), 2.93–2.82 (m, 2H), 2.54–2.45 (m, 1H), 2.37–2.30 (m, 1H), 2.02 (m,

2H), 1.82 (m, 2H), 1.46 (s, 9H).

4.1.57. Synthesis of 1-(3-(1-methyl-2,6-dioxopiperidin-3-yl)-4-oxo-3,4-dihydrobenzo[d][1,2,3]triazin-6-yl)piperidine-4-carboxylic acid (**38**)

Similar procedure of **20a** was performed to give **38** as crude white solid. The crude product was used in the next step without purification.

4.1.58. Synthesis of *N*-((1*r*,3*r*)-3-(3-chloro-4-cyanophenoxy)-2,2,4,4-tetramethylcyclobutyl)-4-(4-(7-(1-(3-(1-methyl-2,6-dioxopiperidin-3-yl)-4-oxo-3,4-dihydrobenzo[d][1,2,3]triazin-6-yl)piperidine-4-carbonyl)-7-azaspiro[3.5]nonan-2-yl)piperazin-1-yl)benzamide (**39**)

To a solution of **28b** (15 mg, 0.0239 mmol), **38** (14 mg, 0.0359 mmol), EDCl·HCl (5 mg, 0.0262 mmol), and HOBt (4 mg, 0.0262 mmol) in DMF (2 mL) was added DIPEA (0.021 mL, 0.119 mmol). The reaction mixture was stirred at room temperature for 12 h. The reaction mixture was diluted with water and extracted with ethyl acetate. The organic layer was washed with brine, dried over Na₂SO₄ and concentrated under reduced pressure. The residue was purified by column chromatography to afford **39** (13 mg, 56%) as a white solid. ¹H NMR (500 MHz, CDCl₃) δ 7.99 (m, 1H), 7.73–7.66 (m, 2H), 7.57 (d, *J* = 8.7 Hz, 1H), 7.52 (d, *J* = 2.7 Hz, 1H), 7.45 (d, *J* = 9.2 Hz, 1H), 6.97 (d, *J* = 2.4 Hz, 1H), 6.95–6.88 (m, 2H), 6.81 (dd, *J* = 8.8, 2.5 Hz, 1H), 6.12 (d, *J* = 8.1 Hz, 1H), 5.78 (dd, *J* = 11.7, 5.4 Hz, 1H), 4.15 (d, *J* = 8.0 Hz, 1H), 4.07 (m, 1H), 4.06–4.02 (m, 2H), 3.59 (m, 1H), 3.53–3.44 (m, 2H), 3.40 (m, 1H), 3.33 (m, 4H), 3.24 (s, 3H), 3.12–3.01 (m, 3H), 2.93–2.82 (m, 2H), 2.84–2.75 (m, 2H), 2.51 (m, 4H), 2.38–2.30 (m, 1H), 2.10 (m, 2H), 1.98–1.82 (m, 6H), 1.76 (m, 2H), 1.67 (m, 1H), 1.57 (m, 1H), 1.26 (s, 6H), 1.22 (s, 6H).

4.2. Biology

4.2.1. Cell culture

VCaP cells were purchased from the American Type Culture Collection (ATCC). LNCaP and 22RV1 cells were purchased from the Korea Research Institute of Bioscience & Biotechnology Bio-Evaluation Center (KRIBB). LNCaP and VCaP cells were grown in IMDM (Invitrogen), and 22RV1 cells were grown in RPMI 1640 (Invitrogen). All of the cells were supplemented with 10% fetal bovine serum (Gibco, #16000–044) and Antibiotic-Antimycotic (Gibco, #15240062) at 37 °C in a humidified 5% CO₂ incubator. DMSO was used as a vehicle.

4.2.2. Western blot analysis

LNCaP and 22RV1 cells were lysed in RIPA buffer (50 mM Tris-HCl, pH7.5, 150 mM NaCl, 1% Triton X-100, 2 mM EDTA, 0.1% SDS, 0.5% sodium deoxycholate and protease inhibitor cocktail) and protein concentration was quantified by Bradford assay. Total protein lysates (30 μg) were separated with SDS-PAGE, and transferred to NC membrane (GE healthcare). The blots were probed with the indicated primary antibodies followed by HRP-conjugated anti-rabbit (Cell signaling, #70745) or anti-mouse IgG antibody (sigma, #A9044). Detection was performed with chemiluminescent HRP substrate (Thermo, #34580). Antibodies for western blots were: *anti*-AR (Santacruz, #sc-7305) and *anti*-tubulin (Sigma, #T5168).

4.2.3. Cell viability assay

LNCaP and VCaP cells were seeded into each well of a 96 well plate with 1.5 × 10³ (LNCaP) and 4 × 10³ (VCaP) cells. Next day, chemicals were treated in each well to a final concentration of 0.3 nM, 1 nM, 3 nM, 10 nM, 30 nM, 100 nM, 300 nM, 1 μM, 3 μM, 10 μM. After 6 days of treatment, cell viability was measured by a CellTiter-Glo (Promega, #G7570) following the manufacturer's

instructions. The viability was quantified compared to DMSO alone. The IC50s were calculated using GraphPad Prism version 6 for Windows. The curves were fitted using a nonlinear regression model with a log (inhibitor) versus response formula.

4.2.4. Liver microsomal metabolic stability

NADPH-dependent metabolism of a test compound in mouse liver microsomes was evaluated. The reaction mixture consisted of liver microsomes (0.5 mg protein/mL) in 100 mM PBS (pH 7.4) and the final concentration of a test compound was 1 μ M. The metabolic reaction was initiated by the addition of NADPH-regenerating solution, containing 1.3 mM NADP⁺, 3.3 mM glucose-6-phosphate, 0.4 U/mL glucose-6-phosphate dehydrogenase, and 3.3 mM MgCl₂. After the 30 min sample incubation at 37 °C, the reaction was stopped by adding ice-cold acetonitrile and the samples were then centrifuged at 13,000 g for 10 min. The supernatant was stored at –20 °C until the analysis.

4.2.5. Pharmacokinetic studies

In male ICR mice (7 weeks), 5 mg/kg, 5 mg/kg and 30 mg/kg of compound were administered via the intravenous (IV), intraperitonea (IP), and oral (PO) route, respectively. The composition of dosing vehicles was 5% DMSO, 52% PEG400, and 3% Tween 80 in water for IV and IP, and 3% Tween8 and 20% PEG400 in water for PO. Blood samples were collected at different time points after drug administration from retro-orbital venous plexus. After obtaining plasma samples by centrifugation of blood samples, protein precipitation was performed by adding acetonitrile at a 1:10 sample dilution. After vortex mixing and centrifugation, the supernatant was collected and analyzed by LC-MS/MS. Mean plasma concentration-time data were analyzed using noncompartmental methods (Phoenix WinNonlin software, Pharsight Corporation, Mountain View, CA). Standard pharmacokinetic parameters were calculated and included maximal plasma concentration (C_{max}), time to reach C_{max} (T_{max}), area under the plasma concentration-time curve from time 0 to time of last measurable concentration (AUC_{last}), area under the plasma concentration-time curve from time 0 to infinity (AUC_{inf}), half-life (T_{1/2}), clearance rate (CL), and volume of distribution (Vd_{ss}). The bioavailability (F) was calculated as (AUC_{non-intravenous} × dose_{i.v.})/(AUC_{i.v.} × dose_{non-intravenous}).

4.2.6. In vivo xenograft assay

SCID mice (C-B-17/lcrCrj-scid, male) were obtained from Charles River of Japan. Animals were maintained under clean room conditions in sterile filter top cages and housed on high efficiency particulate air-filtered ventilated racks. Animals were received sterile rodent chow and water ad libitum. All of the procedures were conducted in accordance with guidelines approved by the Laboratory Animal Care and Use Committee of Korea Research Institute of Chemical Technology. VCaP cells (1.5 × 10⁷ cells + matrigel (Corning Life Science) (1:1)/mouse) were implanted subcutaneously into the right flank region of each mouse and allowed to grow to the designated size. Once tumors reached an average volume of about 130 mm³, mice were dosed via intraperitoneal daily with the indicated doses of vehicle (20% PEG400 + 3% Tween 80 in PBS) or TD-802 for 10 days. Mice were observed daily throughout the treatment period for signs of morbidity/mortality. Tumors were measured twice weekly using calipers, and volume was calculated using the formula: length × width² × 0.5. Body weight was also assessed twice weekly. Statistical significances were evaluated by using Mann-Whitney U test (α = 0.01).

Author contributions

ADT, YUJ, HSK, CHS synthesized compounds. SHJ conducted

biology experiments. SA, HJK, HKL, COL designed and conducted some experiments. JHK, and JYH wrote the manuscript. JDH, JHK, and JYH contributed to experimental design and supervision.

Declaration of competing interest

The authors declare that they have no known competing financial interests or personal relationships that could have appeared to influence the work reported in this paper.

Acknowledgements

This work was supported by the grant (CAP-15-11-KRICT) from National Research Council of Science and Technology, the grant (NRF-2019M3E5D4069882) from the National Research Foundation, Ministry of Science and ICT and future planning, and the grant from the KRIBB Initiative program.

Appendix A. Supplementary data

Supplementary data to this article can be found online at <https://doi.org/10.1016/j.ejmech.2020.112769>.

References

- [1] S. Davison, R. Bell, Androgen physiology, *Semin. Reprod. Med.* 24 (2006) 71–77.
- [2] N.Z. Lu, S.E. Wardell, K.L. Burnstein, D. Defranco, P.J. Fuller, V. Giguere, R.B. Hochberg, L. McKay, J.-M. Renoir, N.L. Weigel, E.M. Wilson, D.P. McDonnell, J.A. Cidlowski, International Union of Pharmacology. LXV, The pharmacology and classification of the nuclear receptor superfamily: glucocorticoid, mineralocorticoid, progesterone, and androgen receptors, *Pharmacol. Rev.* 58 (2006) 782–797.
- [3] A.D. Mooradian, J.E. Morley, S.G. Korenman, Biological actions of androgens, *Endocr. Rev.* 8 (1987) 1–28.
- [4] C.A. Heinlein, C. Chang, The roles of androgen receptors and androgen-binding proteins in nongenomic androgen actions, *Mol. Endocrinol.* 16 (2002) 2181–2187.
- [5] P.L. Palmbo, M. Hussain, Non-castrate metastatic prostate cancer: have the treatment options changed? *Semin. Oncol.* 40 (2013) 337–346.
- [6] M.E. Tan, J. Li, H.E. Xu, K. Melcher, E.L. Yong, Androgen receptor: structure, role in prostate cancer and drug discovery, *Acta Pharmacol. Sin.* 36 (2015) 3–23.
- [7] M. Sanford, Enzalutamide : a review of its use in metastatic , castration-resistant prostate cancer, *Drugs* 73 (2013) 1723–1732.
- [8] T. Karantanos, P.G. Corn, T.C. Thompson, Prostate cancer progression after androgen deprivation therapy : mechanisms of castrate resistance and novel therapeutic approaches, *Oncogene* 32 (2013) 5501–5511.
- [9] D.E. Rathkopf, H.I. Scher, Apalutamide for the treatment of prostate cancer, *Expert Rev. Anticancer Ther.* 18 (2018) 823–836.
- [10] R. Narayanan, S. Ponnusamy, D.D. Miller, Destroying the androgen receptor (AR) –potential strategy to treat advanced prostate cancer, *Oncoscience* 4 (2017) 175–177.
- [11] K.M. Sakamoto, K.B. Kim, A. Kumagai, F. Mercurio, C.M. Crews, R.J. Deshaies, Protacs : chimeric molecules that target proteins to the Skp 1 – Cullin – F box complex for ubiquitination and degradation, *Proc. Natl. Acad. Sci. U.S.A.* 98 (2001) 8554–8559.
- [12] M. Toure, C.M. Crews, Small-molecule PROTACS: new approaches to protein degradation, *Angew. Chem. Int. Ed.* 55 (2016) 1966–1973.
- [13] A.C. Lai, C.M. Crews, Induced protein degradation: an emerging drug discovery paradigm, *Nat. Rev. Drug Discov.* 16 (2017) 101–114.
- [14] X. Sun, J. Wang, X. Yao, W. Zheng, Y. Mao, T. Lan, L. Wang, Y. Sun, X. Zhang, Q. Zhao, J. Zhao, R. Xiao, X. Zhang, G. Ji, Y. Rao, A chemical approach for global protein knockdown from mice to non-human primates, *Cell Discov* 5 (2019) 1–10.
- [15] J. Hu, B. Hu, M. Wang, F. Xu, B. Miao, C.-Y. Yang, M. Wang, Z. Liu, D.F. Hayes, K. Chinnaswamy, J. Delproposto, J. Stuckey, S. Wang, Discovery of ERD-308 as a highly potent proteolysis targeting chimera (PROTAC) degrader of estrogen receptor (ER), *J. Med. Chem.* 62 (2019) 1420–1442.
- [16] R.B. Kargbo, PROTAC-mediated degradation of estrogen receptor in the treatment of cancer, *ACS Med. Chem. Lett.* 10 (2019) 1367–1369.
- [17] X. Han, L. Zhao, W. Xiang, C. Qin, B. Miao, T. Xu, M. Wang, C.-Y. Yang, K. Chinnaswamy, J. Stuckey, S. Wang, Discovery of highly potent and efficient PROTAC degraders of androgen receptor (AR) by employing weak binding affinity VHL E3 ligase ligands, *J. Med. Chem.* 62 (2019) 11218–11231.
- [18] H. Zhang, G. Li, Y. Zhang, J. Shi, B. Yan, H. Tang, S. Chen, J. Zhang, P. Wen, Z. Wang, C. Pang, J. Li, W. Guo, S. Zhang, Targeting BET proteins with a PROTAC molecule elicits potent anticancer activity in HCC cells, *Front. Oncol.* 9 (2020)

- 1–11.
- [19] G.M. Burslem, A.R. Schultz, D.P. Bondeson, C.A. Eide, S.L. Savage Stevens, B.J. Druker, C.M. Crews, Targeting BCR-ABL1 in chronic myeloid leukemia by PROTAC-mediated targeted protein degradation, *Canc. Res.* 79 (2019) 4744–4753.
- [20] A. Mares, A.H. Miah, I.E.D. Smith, M. Rackham, A.R. Thawani, J. Cryan, P.A. Haile, B.J. Votta, A.M. Beal, C. Capriotti, M.A. Reilly, D.T. Fisher, N. Zinn, M. Bantscheff, T.T. MacDonald, A. Vossenkamper, P. Dace, I. Churcher, A.B. Benowitz, G. Watt, J. Denyer, P. Scott-Stevens, J.D. Harling, Extended pharmacodynamic responses observed upon PROTAC-mediated degradation of RIPK2, *Commun. Biol.* 3 (2020) 1–13.
- [21] See the link, <https://clinicaltrials.gov/ct2/results?cond=Prostate+Cancer&term=ARV-110&cntry=&state=&city=&dist=>.
- [22] N. Shibata, K. Nagai, Y. Morita, O. Ujikawa, N. Ohoka, T. Hattori, R. Koyama, O. Sano, Y. Imaeda, H. Nara, N. Cho, M. Naito, Development of protein degradation inducers of androgen receptor by conjugation of androgen receptor ligands and inhibitor of apoptosis protein ligands, *J. Med. Chem.* 61 (2018) 543–575.
- [23] J. Salami, S. Alabi, R.R. Willard, N.J. Vitale, J. Wang, H. Dong, M. Jin, D.P. McDonnell, A.P. Crew, T.K. Neklesa, C.M. Crews, Androgen receptor degradation by the proteolysis-targeting chimera ARCC-4 outperforms enzalutamide in cellular models of prostate cancer drug resistance, *Commun. Biol.* 1 (2018) 100.
- [24] X. Han, C. Wang, C. Qin, W. Xiang, E. Fernandez-Salas, C.-Y. Yang, M. Wang, L. Zhao, T. Xu, K. Chinnaswamy, J. Delproposito, J. Stuckey, S. Wang, Discovery of ARD-69 as a highly potent proteolysis targeting chimera (PROTAC) degrader of androgen receptor (AR) for the treatment of prostate cancer, *J. Med. Chem.* 62 (2019) 941–964.
- [25] S.A. Kim, A. Go, S. Jo, S.J. Park, Y.U. Jeon, J.E. Kim, H.K. Lee, C.H. Park, C. Lee, S.G. Park, P. Kim, B.C. Park, S.Y. Cho, S. Kim, J. Du Ha, J. Kim, J.Y. Hwang, A novel cereblon modulator for targeted protein degradation, *Eur. J. Med. Chem.* 166 (2019) 65–74.
- [26] C. Guo, A. Linton, S. Kephart, M. Ornelas, M. Pairish, J. Gonzalez, S. Greasley, A. Nagata, B.J. Burke, M. Edwards, N. Hosea, P. Kang, W. Hu, J. Engebretsen, D. Briere, M. Shi, H. Gukasyan, P. Richardson, K. Dack, T. Underwood, P. Johnson, A. Morell, R. Felstead, H. Kuruma, H. Matsumoto, A. Zoubeidi, M. Gleave, G. Los, A.N. Fanjul, Discovery of aryloxy tetramethylcyclobutanes as novel androgen receptor antagonists, *J. Med. Chem.* 54 (2011) 7693–7704.
- [27] K. Pereira de Jesus-Tran, P.-L. Côté, L. Cantin, J. Blanchet, F. Labrie, R. Breton, Comparison of crystal structures of human androgen receptor ligand-binding domain complexed with various agonists reveals molecular determinants responsible for binding affinity, *Protein Sci.* 15 (2006) 987–999.
- [28] K. Cyrus, M. Wehenkel, E. Choi, H. Han, H. Lee, H. Swanson, K. Kim, Impact of linker length on the activity of PROTACs, *Mol. Biosyst.* 7 (2011) 359–364.
- [29] D.P. Bondeson, B.E. Smith, G.M. Burslem, A.D. Buhimschi, J. Hines, S. Jaime-Figueroa, J. Wang, B.D. Hamman, A. Ishchenko, C.M. Crews, Lessons in PROTAC design from selective degradation with a promiscuous warhead, *Cell Chem. Biol.* 25 (2018) 78–87.
- [30] J. Luo, G. Attard, S.P. Balk, C. Bevan, K. Burnstein, L. Cato, A. Cherkasov, J.S. De Bono, Y. Dong, A.C. Gao, M. Gleave, H. Heemers, M. Kanayama, R. Kittler, J.M. Lang, R.J. Lee, C.J. Logothetis, R. Matusik, S. Plymate, C.L. Sawyers, L.A. Selth, H. Soule, W. Tilley, N.L. Weigel, A. Zoubeidi, S.M. Dehm, G.V. Raj, Role of androgen receptor variants in prostate cancer: report from the 2017 mission androgen receptor variants meeting, *Eur. Urol.* 73 (2018) 715–723.